TKK Dissertations 52
Espoo 2006

FUNCTIONAL MATERIALS BASED ON SELF-ASSEMBLED COMB-SHAPED SUPRAMOLECULES

Doctoral Dissertation

Sami Valkama

Helsinki University of Technology
Department of Engineering Physics and Mathematics
Optics and Molecular Materials

TKK Dissertations 52
Espoo 2006

FUNCTIONAL MATERIALS BASED ON SELF-ASSEMBLED COMB-SHAPED SUPRAMOLECULES

Doctoral Dissertation

Sami Valkama

Dissertation for the degree of Doctor of Science in Technology to be presented with due permission of the Department of Engineering Physics and Mathematics for public examination and debate in Auditorium F1 at Helsinki University of Technology (Espoo, Finland) on the 8th of December, 2006, at 12 noon.

Helsinki University of Technology
Department of Engineering Physics and Mathematics
Optics and Molecular Materials

Teknillinen korkeakoulu
Teknillisen fysiikan ja matematiikan osasto
Optiikka ja molekyylimateriaalit

Distribution:
Helsinki University of Technology
Department of Engineering Physics and Mathematics
Optics and Molecular Materials
P.O. Box 2200
FI - 02015 TKK
FINLAND
URL: http://omm.tkk.fi/
Tel. +358-9-451 3153
Fax. +358-9-451 3155
E-mail: Sami.Valkama@tkk.fi

ISBN-13 978-951-22-8497-9
ISBN-10 951-22-8497-9
ISBN-13 978-951-22-8498-6 (PDF)
ISBN-10 951-22-8498-7 (PDF)
ISSN 1795-2239
ISSN 1795-4584 (PDF)
URL: http://lib.tkk.fi/Diss/2006/isbn9512284987/

TKK-DISS-2219

Otamedia Oy
Espoo 2006

HELSINKI UNIVERSITY OF TECHNOLOGY P. O. BOX 1000, FI-02015 TKK http://www.tkk.fi	ABSTRACT OF DOCTORAL DISSERTATION

Author Sami Valkama

Name of the dissertation: Functional materials based on self-assembled comb-shaped supramolecules

Date of manuscript August 22th, 2006	Date of the dissertation December 8th 2006

☐ Monograph ☒ Article dissertation (summary + original articles)

Department	Department of Engineering Physics and Mathematics
Laboratory	Optics and Molecular Materials
Field of research	Engineering Physics / Polymer Physics
Opponent(s)	Prof. Dr. Raffaele Mezzenga
Supervisor	Prof. Olli Ikkala
Instructor	Academy Research Fellow Janne Ruokolainen

Abstract

In this Thesis self-assembly of comb-shaped supramolecules, i.e., polymer-amphiphile complexes and hierarchical self-assembly of comb-coil supramolecules, i.e., block copolymer amphiphile complexes are studied. The comb-shaped architecture leads to stretching of chains and the amphiphilic side chains act as plastizicers providing better local structures even with high molecular weight samples. This enables to prepare photonic bandgap materials, which show a reversible and large bandgap switching in a narrow temperature range. In addition, the use of physical interactions instead of covalent enables the cleavage of entities once the structure is formed, leading to porous materials. In this Thesis two template-assisted approaches towards functional porous polymeric materials are described, i.e., selective extraction of coordinated amphiphiles and controlled pyrolysis of block copolymer in the presence of phenolic resin.

This Thesis consists of an overview of the following 8 publications:

1. S. Valkama, T. Ruotsalainen, A. Nykänen, A. Laiho, H. Kosonen, G. ten Brinke, O. Ikkala, J. Ruokolainen, Macromolecules 2006, in press.
2. S. Valkama, O. Lehtonen, K. Lappalainen, H. Kosonen, P. Castro, T. Repo, M. Torkkeli, R. Serimaa, G. ten Brinke, M. Leskelä, O. Ikkala, Macromolecular Rapid Communications 2003, 24, 556-560.
3. H. Kosonen, S. Valkama, J. Ruokolainen, M. Torkkeli, R. Serimaa, G. ten Brinke, O. Ikkala, EPJ E 2003, 10, 69 - 75.
4. H. Kosonen, S. Valkama, J. Ruokolainen, M. Torkkeli, R. Serimaa, G. ten Brinke, O. Ikkala, MRS Symposium Proceedings 2003, 775, P6.18.1 – P6.18.6.
5. S. Valkama, H. Kosonen, J. Ruokolainen, T. Haatainen, M. Torkkeli, R. Serimaa, G. ten Brinke, O. Ikkala, Nat. Mater. 2004, 3, 872 - 876.
6. S. Valkama, T. Ruotsalainen, H. Kosonen, J. Ruokolainen, M. Torkkeli, R. Serimaa, G. ten Brinke, O. Ikkala, Macromolecules 2003, 36, 3986-3991.
7. H. Kosonen, S. Valkama, A. Nykänen, M. Toivanen, G. ten Brinke, J. Ruokolainen, O. Ikkala, Adv. Mater. 2006, 18, 201 – 205.
8. S.Valkama, A. Nykänen, H. Kosonen, R. Ramani, F. Tuomisto, P. Engelhardt, G. ten Brinke, O. Ikkala, J. Ruokolainen, Adv. Funct. Mater. 2006, in press.

Keywords self-assembly, functional material, polymer, photonic bandgap, porous material

ISBN (printed) 951-22-8497-9	ISSN (printed) 1795-2239
ISBN (pdf) 951-22-8498-7	ISSN (pdf) 1795-4584
ISBN (others)	Number of pages 56 + app. 78

Publisher

Print distribution Optics and molecular materials

☒ The dissertation can be read at http://lib.tkk.fi/Diss/2006/isbn9512284987/

TEKNILLINEN KORKEAKOULU PL 1000, 02015 TKK http://www.tkk.fi	VÄITÖSKIRJAN TIIVISTELMÄ

Tekijä Sami Valkama

Väitöskirjan nimi: Itsejärjestyneisiin kampamaisiin supramolekyyleihin perustuvat funktionaaliset materiaalit

Käsikirjoituksen jättämispäivämäärä 22.8.2006	Väitöstilaisuuden ajankohta 8.12.2006

☐ Monografia ☒ Yhdistelmäväitöskirja (yhteenveto + erillisartikkelit)

Osasto	Teknillisen fysiikan ja matematiikan osasto
Laboratorio	Optiikka ja molekyylimateriaalit
Tutkimusala	Teknillinen fysiikka / Polymeerifysiikka
Vastaväittäjä(t)	Prof. Dr. Raffaele Mezzenga
Työn valvoja	Prof. Olli Ikkala
Työn ohjaaja	Akatemian tutkija Janne Ruokolainen

Tiivistelmä

Tässä väitöskirjassa tutkitaan kampamaisten supramolekyylien itsejärjestymistä. Kampamainen rakenne aiheuttaa polymeeriketjujen venymistä ja samanaikaisesti amfifiiliset sivuketjut plastisoivat materiaalia mahdollistaen hyvin järjestyneiden polymeerirakenteiden aikaansaamisen jopa korkeilla molekyylipainoilla. Tätä voidaan hyödyntää valmistettaessa polymeerifotonikiteitä, joita tässä väitöskirjassa on tutkittu. Toisaalta fysikaaliset vuorovaikutukset polymeerin ja amfifiilin välillä mahdollistavat supramolekulaarisen templaatin poistamisen rakenteiden muodostumisen jälkeen, jolloin jäljelle jää huokoisia materiaaleja. Tässä väitöskirjassa on tutkittu kahta erilaista tapaa valmistaa huokoisia materiaaleja: koordinoitujen amfifiilien poistaminen selektiivisellä liuottimella ja lohkopolymeeri/fenolihartsikompleksien kontrolloitu pyrolysointi.

Väitöskirja koostuu seuraavista kahdeksasta julkaisusta:

1. S. Valkama, T. Ruotsalainen, A. Nykänen, A. Laiho, H. Kosonen, G. ten Brinke, O. Ikkala, J. Ruokolainen, Macromolecules 2006, painossa.
2. S. Valkama, O. Lehtonen, K. Lappalainen, H. Kosonen, P. Castro, T. Repo, M. Torkkeli, R. Serimaa, G. ten Brinke, M. Leskelä, O. Ikkala, Macromolecular Rapid Communications 2003, 24, 556-560.
3. H. Kosonen, S. Valkama, J. Ruokolainen, M. Torkkeli, R. Serimaa, G. ten Brinke, O. Ikkala, EPJ E 2003, 10, 69 - 75.
4. H. Kosonen, S. Valkama, J. Ruokolainen, M. Torkkeli, R. Serimaa, G. ten Brinke, O. Ikkala, MRS Symposium Proceedings 2003, 775, P6.18.1 – P6.18.6.
5. S. Valkama, H. Kosonen, J. Ruokolainen, T. Haatainen, M. Torkkeli, R. Serimaa, G. ten Brinke, O. Ikkala, Nat. Mater. 2004, 3, 872 - 876.
6. S. Valkama, T. Ruotsalainen, H. Kosonen, J. Ruokolainen, M. Torkkeli, R. Serimaa, G. ten Brinke, O. Ikkala, Macromolecules 2003, 36, 3986-3991.
7. H. Kosonen, S. Valkama, A. Nykänen, M. Toivanen, G. ten Brinke, J. Ruokolainen, O. Ikkala, Adv. Mater. 2006, 18, 201–205.
8. S.Valkama, A. Nykänen, H. Kosonen, R. Ramani, F. Tuomisto, P. Engelhardt, G. ten Brinke, O. Ikkala, J. Ruokolainen, Advanced Functional Materials 2006, painossa.

Asiasanat itsejärjestyminen, funktionaalinen materiaali, polymeeri, fotonikide, huokoinen materiaali

ISBN (painettu) 951-22-8497-9	ISSN (painettu) 1795-2239
ISBN (pdf) 951-22-8498-7	ISSN (pdf) 1795-4584
ISBN (muut)	Sivumäärä 56 + liit. 78

Julkaisija

Painetun väitöskirjan jakelu Optiikka ja molekyylimateriaalit

☒ Luettavissa verkossa osoitteessa http://lib.tkk.fi/Diss/2006/isbn9512284987/

PREFACE

This work has been carried out in the Centre of Excellence of Academy of Finland ("Bio- and Nanopolymer Research group", 77317) at the Department of Engineering Physics and Mathematics at Helsinki University of Technology under supervision of Prof. Olli Ikkala and Academy Research Fellow Janne Ruokolainen. I would like to thank them for the encouragement as well as the enthusiasm and endless stream of new ideas. Prof. Gerrit ten Brinke, thanks for the numerous discussions and help along the way.

I wish to thank the important collaborators Prof. Ritva Serimaa and PhD Mika Torkkeli for helpful discussions and their expertise in X-ray scattering. Many thanks also to collaborators in Helsinki University (Prof. Heikki Tenhu, Prof. Markku Leskelä, Doc. Timo Repo, PhD Pascal Castro, and PhD Kristian Lappalainen), in Technical Research Centre of Finland (Lic.Sc. Tapio Mäkelä and M.Sc. Tomi Haatainen), in Polytechnic University of Brooklyn (Prof. Kalle Levon) and in Helsinki University of Technology (Prof. Jukka Seppälä and M.Sc. Kati Vilonen) for sharing the information and facilities.

All the former and present members of the research group deserve my thanks for making the laboratory such a nice working environment. Especially, I want to express my thanks to PhD Harri Kosonen and M.Sc. Teemu Ruotsalainen for the excellent collaboration. Secretary Orvokki Nyberg I thank for all help. Special thanks: Jani, for your friendship along the way and for paving me the way to new challenges. M.Sc. Matti Kaarnakari, for your friendship and the nice time at golf course. Peräkylän Ponnistus and especially Suinulan Teräsmies for keeping me fit.

Grants from the Foundation of Technology, the Kemira Foundation, the Orion Foundation, the Jenny and Antti Wihuri foundation, the Emil Aaltonen Foundation, the Heikki and Hilma Honkanen foundation, and the Väisälä Foundation are gratefully acknowledged. The research was funded by the National Technology Agency and the Academy of Finland.

Finally, I wish to thank my parents and brothers for their support and encouragement over the years. Especially, Kati and Veeti, thank you for just being there for me!

Espoo, November 2006

Sami Valkama

LIST OF PUBLICATIONS

I **Sami Valkama**, Teemu Ruotsalainen, Antti Nykänen, Ari Laiho, Harri Kosonen, Gerrit ten Brinke, Olli Ikkala, and Janne Ruokolainen. *Self-Assembled Structures in Diblock Copolymers with Hydrogen-Bonded Amphiphilic Plasticizing Compounds,* Macromolecules **2006**, in press.

II **Sami Valkama**, Olli Lehtonen, Kristian Lappalainen, Harri Kosonen, Pascal Castro, Timo Repo, Mika Torkkeli, Ritva Serimaa, Gerrit ten Brinke, Markku Leskelä, and Olli Ikkala. *Multicomb Polymeric Supramolecules and Their Self-Organization: Combination of Coordination and Ionic Interactions,* Macromolecular Rapid Communications **2003**, 24, 556 – 560.

III Harri Kosonen, **Sami Valkama**, Janne Ruokolainen, Mika Torkkeli, Ritva Serimaa, Gerrit ten Brinke, and Olli Ikkala. *One-Dimensional Optical Reflectors Based on Self-Organization of Polymeric Comb-Shaped Supramolecules,* The European Physical Journal E **2003**, 10, 69 – 75.

IV Harri Kosonen, **Sami Valkama**, Janne Ruokolainen, Mika Torkkeli, Ritva Serimaa, Gerrit ten Brinke, and Olli Ikkala. *Polymeric One-Dimensional Reflectors Based on Self-Organization of Comb-Shaped Supramolecules,* Material Research Society Symposium Proceedings **2003**, 775, P6.18.1 – P6.18.6.

V **Sami Valkama**, Harri Kosonen, Janne Ruokolainen, Tomi Haatainen, Mika Torkkeli, Ritva Serimaa, Gerrit ten Brinke, and Olli Ikkala. *Self-Assembled Polymeric Solid Films with Temperature-Induced Large and Reversible Photonic-Bandgap Switching,* Nature Materials **2004**, 3, 872 – 876.

VI **Sami Valkama**, Teemu Ruotsalainen, Harri Kosonen, Janne Ruokolainen, Mika Torkkeli, Ritva Serimaa, Gerrit ten Brinke, and Olli Ikkala. *Amphiphiles Coordinated to Block Copolymer as a Template for Mesoporous Materials,* Macromolecules **2003**, 36, 3986 – 3991.

VII Harri Kosonen, **Sami Valkama**, Antti Nykänen, Miika Toivanen, Gerrit ten Brinke, Janne Ruokolainen, and Olli Ikkala. *Functional Porous Structures Based on the Pyrolysis of Cured Templates of Block Copolymer and Phenolic Resin*, Advanced Materials **2006**, 18, 201 – 205.

VIII **Sami Valkama**, Antti Nykänen, Harri Kosonen, R. Ramani, Filip Tuomisto, Peter Engelhardt, Gerrit ten Brinke, Olli Ikkala, and Janne Ruokolainen. *Hierarchical Porosity in Self-Assembled Polymers: Post-Modification of Block Copolymer - Phenolic Resin Complexes by Pyrolysis Allows the Control of Micro- and Mesoporosity*, Advanced Functional Materials **2006**, in press.

Alongside this Thesis, the author has contributed several other publications and patent, which are directly related to this Thesis:

1. **Sami Valkama**, Riikka Mäki-Ontto, Manfred Stamm, Gerrit ten Brinke, and Olli Ikkala. *Mesoporous Polymeric Materials Based on Comb-Coil Supramolecules,* Studied in Surface Science and Catalysis **2002**, 141, 371 – 378.
2. Harri Kosonen, **Sami Valkama**, Juha Hartikainen, Hannele Eerikäinen, Mika Torkkeli, Kaija Jokela, Ritva Serimaa, Franciska Sundholm, Gerrit ten Brinke, and Olli Ikkala. *Mesomorphic Structure of Poly(styrene)-block-poly(4-vinylpyridine) with Oligo(ethylene oxide)sulfonic acid side chains as a Model for Molecularly Reinforced Polymer Electrolyte*, Macromolecules **2002**, 35, 10149 – 10154.
3. Harri Kosonen, **Sami Valkama**, Janne Ruokolainen, Matti Knaapila, Mika Torkkeli, Ritva Serimaa, Andrew P. Monkman, Gerrit ten Brinke, and Olli Ikkala. *Processible Conducting Nanoscale Cylinders due to Self-Organized Polyaniline Supramolecules*, Synthetic Metals **2002**, 137, 881 – 882.
4. **Sami Valkama**, Juha Hartikainen, Mika Torkkeli, Ritva Serimaa, Janne Ruokolainen, Kari Rissanen, Gerrit ten Brinke, and Olli Ikkala. *Self-Organized Nanostructures of Poly(4-vinylpyridine), Polyaniline and Polyamides due to Metal Complexation,* Macromolecular Symposia **2002**, 186, 87 – 92.
5. Juha Hartikainen, Olli Lehtonen, Tapio Harmia, Mathias Lindner, **Sami Valkama**, Janne Ruokolainen, and Klaus Friedrich. *Structure and Morphology of Polyamide 66 and Oligomeric Phenolic Resin Blends: Molecular Modeling and Experimental Investigations*, Chemistry of Materials **2004**, 16, 3032 – 3039.
6. Ali Harlin, Olli Ikkala, Harri Kosonen, **Sami Valkama**, Teemu Ruotsalainen, Riikka Mäki-Ontto, Jani Turku, Janne Ruokolainen, and Pirjo Heikkilä. *A Method for Manufacturing a Fibrous Structure, a Method for Manufacturing a Fiber, and a Fibrous Structure*, PCT Int. Appl. **2005**, WO 2005049707, 36 pp.
7. Arri Priimägi, Stefano Cattaneo, Robin H. A. Ras, **Sami Valkama**, Olli Ikkala, and Martti Kauranen. *Polymer-Dye Complexes: Supramolecular Route Toward Functional Optical Materials*, Chemistry of Materials **2005,** 17(23), 5798 – 5802.
8. Ari Laiho, Robin H. A. Ras, **Sami Valkama**, Janne Ruokolainen, Ronald Österbacka, and Olli Ikkala. *Control of Self-Assembly by Charge-Transfer Complexation between C_{60} Fullerene and Electron Donating Units of Block Copolymers*, Macromolecules **2006**, 39, 7648 – 7653.
9. Arri Priimägi, Stefano Cattaneo, Robin H. A. Ras, **Sami Valkama**, Olli Ikkala, and Martti Kauranen. *Supramolecular guest-host systems: combining high dye doping level with low aggregation tendency*, Proceedings of SPIE **2006**, 61922U/1 – 61922U/8.

AUTHOR'S CONTRIBUTION

The research reported in this Thesis is the result of a group work carried out during years 2001 – 2006 in the laboratory of Optics and Molecular Materials at Helsinki University of Technology in collaboration with Prof. Gerrit ten Brinke from the University of Groningen.

The author has taken active part in all stages of the design, realization, analysis, and reporting of the work presented in this Thesis. The author has written the first versions of Publications II – VIII. In Publication I author has an equal contribution with Teemu Ruotsalainen in all stages of the Publication.

The small angle X-ray scattering studies (SAXS) reported in Articles I, III, and V – VIII were carried out at the Dutch-Belgian beamline (BM26B) of European Synchrotron Radiation Facility in Grenoble. Additional SAXS measurements in Articles II, III, V, and VI were performed at the University of Helsinki in collaboration with Prof. Ritva Serimaa and PhD Mika Torkkeli. The quantum chemical calculations reported in Article II were done by M.Sc. Olli Lehtonen from the Department of Engineering Physics and Mathematics at Helsinki University of Technology. The AFM and TEM images represented in Articles IV and V have been done in collaboration with Academy Research Fellow Janne Ruokolainen at the Department of Materials at the University of California Santa Barbara. M.Sc. Kati Vilonen from the Department of Chemical Technology at Helsinki University of Technology was responsible for the surface area measurements reported in Articles VII and VIII. Positron annihilation lifetime spectroscopy measurements in Article VIII were performed by PhD R. Ramani from the Department of Engineering Physics and Mathematics at Helsinki University of Technology. The 3D transmission electron tomography shown in Article VIII has been realized in collaboration with Docent Peter Engelhardt from the Laboratory of Computational Engineering at Helsinki University of Technology.

The author has also presented the results covered in this Thesis at several international conferences.

CONTENTS

1. BACKGROUND

1.1. Introduction

Nanometer scale structures and patterning have become important in order to meet the increasing demand for functional and "smart" matter and smaller and faster devices. Lithographic techniques (a "*top-down*" approach) enable processing of periodic and aperiodic features with high accuracy below 100 nm. However, lithographic methods are usually restricted to 2D or require expensive instrument or long writing times. Another approach towards nanometer scale structures is to use self-assembly[1] [1-3] ("*bottom-up"* approach), in which competing attractive and repulsive forces within a molecular system are balanced. In polymers, a typical example consists of block copolymers, where chemically distinct polymer chains are covalently bonded to each other to form single molecules [4-12]. Owing to their mutual repulsion, dissimilar blocks tend to segregate into different domains. In the simplest case of non-crystalline flexible coil diblock copolymers, e.g. lamellar, gyroid, cylindrical or spherical phases are formed, depending on the volume fractions of the blocks and χN [13-15].[2] More complicated structures are achieved if more blocks or different architectures, such as star-shape (mictoarm) or dendritic shapes copolymers, are used [13, 16-21] [22]. These two approaches, i.e. *"bottom-up"* and *"top-down"*, are merged in directed self-assembly, where e.g. topographic features or chemically patterned surfaces and external fields have been used to direct the self-assembly process [23].

Other examples of self-assembled polymeric structures are comb-shaped supramolecules (for supramolecular chemistry see Ref. [7, 24]), where amphiphilic[3] molecules are attached to polymer backbone by physical interactions (Figure 1) instead of covalent bonding. Structure formation and phase behaviour are mainly affected by the attraction strength of the polymer-amphiphile interaction and repulsion between the polar polymer backbone and non-polar alkyl tails. Complexes using different well-balanced polymer-amphiphile interactions have been introduced, i.e. by ionic bonds [8, 10-12, 25-36] [37-42], coordination [5, 43-49], hydrogen bonds [50-61] or combination of different physical interactions [51, 62]. Usually polymer-amphiphile complexes form lamellar or cylindrical structures with the long period of ca. 2 – 5 nm [27, 63-66], but in some cases also more complex morphologies are obtained [10, 27, 63, 67]. The supramolecular side chains can also be mesogenic, as in supramolecular side chain liquid crystalline polymers [32, 35, 60, 61, 68-71].

[1] In this Thesis expression self-assembly is used as a synonym for microphase separation and self-organization. In articles II-V self-organization is used instead of self-assembly due to anachronistic terminology. However, in thermodynamics self-organization sometimes refers to dissipative structure formation requiring energy input to form and maintain the structure [1-2]. Therefore, in this Thesis self-assembly refers to the spontaneous structure formation due to competing attractive and repulsive interactions in the fluid, glassy or crystalline state. Self-assembly can also be static and dynamic [3].

[2] χ is the Flory-Huggins interaction parameter between blocks and N is the total degree of polymerisation of diblock copolymer (equal to the total numbers of A monomers and B monomers).

[3] Within the present context, amphiphilic molecules are low molecular weight compounds with polar head group and non-polar tail group, which usually is aliphatic alkyl chain. Water-soluble amphiphiles are called surfactants.

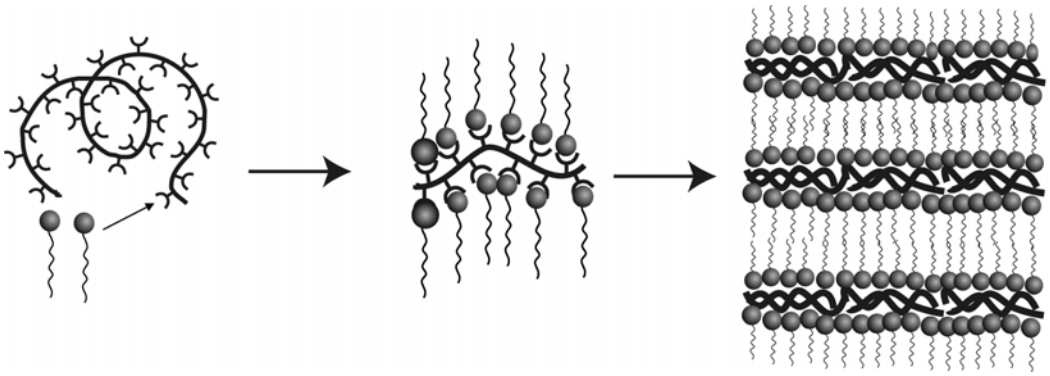

Figure 1. Schematic presentation of the formation of comb-shaped polymer-amphiphile supramolecules and self-assembled lamellar structure.

In supramolecular comb-coil diblock copolymers the self-assembly of polymer-amphiphile complexes is combined with block copolymers, provided that one block of the block copolymer is able to form comb-shaped polymer-amphiphile complex whereas the other is not. Such systems can lead to self-assembly at two different length scales: The larger length scale corresponds to the block copolymer structure (typically 20 – 200 nm) and the shorter length scale is determined by the length of the repulsive side chains within the comb block (typically 2 - 5 nm), see Figure 2. Depending on the volume fractions of the domains and temperature as well as the chemical nature of the side chain, different hierarchical structures are obtained, e.g. lamellar-*within*-lamellar, lamellar-*within*-cylinder, and lamellar-*within*-spheres [51, 52, 72-74]. The low molecular weight amphiphiles can also act as selective solvent or plasticizer promoting faster structure formation and better local structures due to the increased mobility.

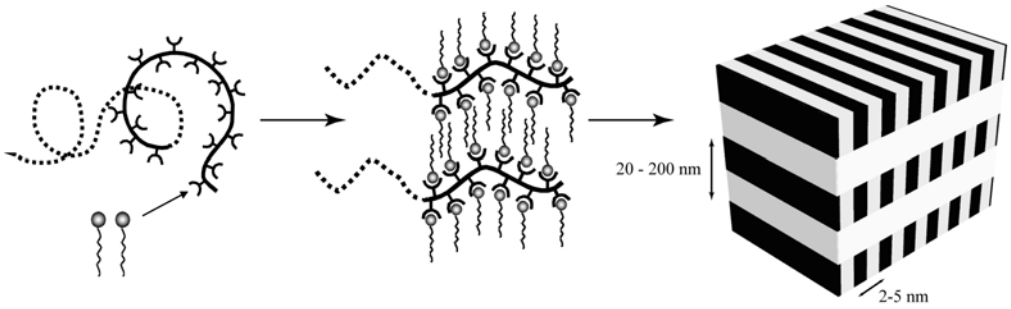

Figure 2. Schematic presentation for a hierarchical self-assembly in supramolecular comb-coil diblock copolymers. The larger block copolymer structure and the smaller polymer-amphiphile structure are typically 20 - 200 nm and 2-5 nm, respectively.

1.2. An outline of the Thesis

In this Thesis self-assembly of comb-shaped supramolecules, i.e., polymer-amphiphile complexes (Figure 1) and hierarchical self-assembly of comb-coil supramolecules, i.e., block copolymer amphiphile complexes (Figure 2) are studied (Articles I – II). These materials can be used to prepare photonic bandgap materials (Articles III – V) or they can be used as a template to construct porous materials by extraction with a selective solvent (Article VI) or by controlled pyrolysis (Articles VII – VIII). The results are presented with a short overview of related work done in the field.

Article I describes hierarchical self-assembly and thermoreversible phase transitions in comb-coil supramolecules consisting of hydrogen bonded side chains. The phase transitions depend on comb-coil diblock copolymer composition, reversibility of the hydrogen bonding, and polymer-solvent phase behavior which enables to achieve reversible transition sequences (in some cases even 5 consecutive phase transitions) that are not easily accessible only by changing the Flory-Huggins interaction parameter χ by temperature, i.e., for example transitions from lamellar to spherical structure. In Article II we show an example how different physical interactions can be combined to form cylindrical self-assembly of multicomb polymeric supramolecules, in which several alkyl chains are connected to each polymeric repeat unit using both coordination and ionic interactions.

The comb-shaped architecture leads to stretching of chains and the amphiphilic side chains act as plastizicers providing better local structures even with high molecular weight samples. In Articles III – IV we describe that these concepts can be used to prepare photonic bandgap materials. Article V represents a system, which shows a reversible and large bandgap switching in a narrow temperature range.

The use of physical interactions instead of covalent enables the cleavage of entities once the structure is formed, leading to porous materials. In Articles VI – VIII two template-assisted approaches towards functional porous polymeric materials are described, i.e., selective extraction of coordinated amphiphiles and controlled pyrolysis of block copolymer in the presence of phenolic resin. Figure 3 summarizes the physical interactions and their combinations used in this Thesis in order to prepare comb-shaped supramolecules and hierarchical self-assembly leading to e.g. photonic bandgap materials and porous materials.

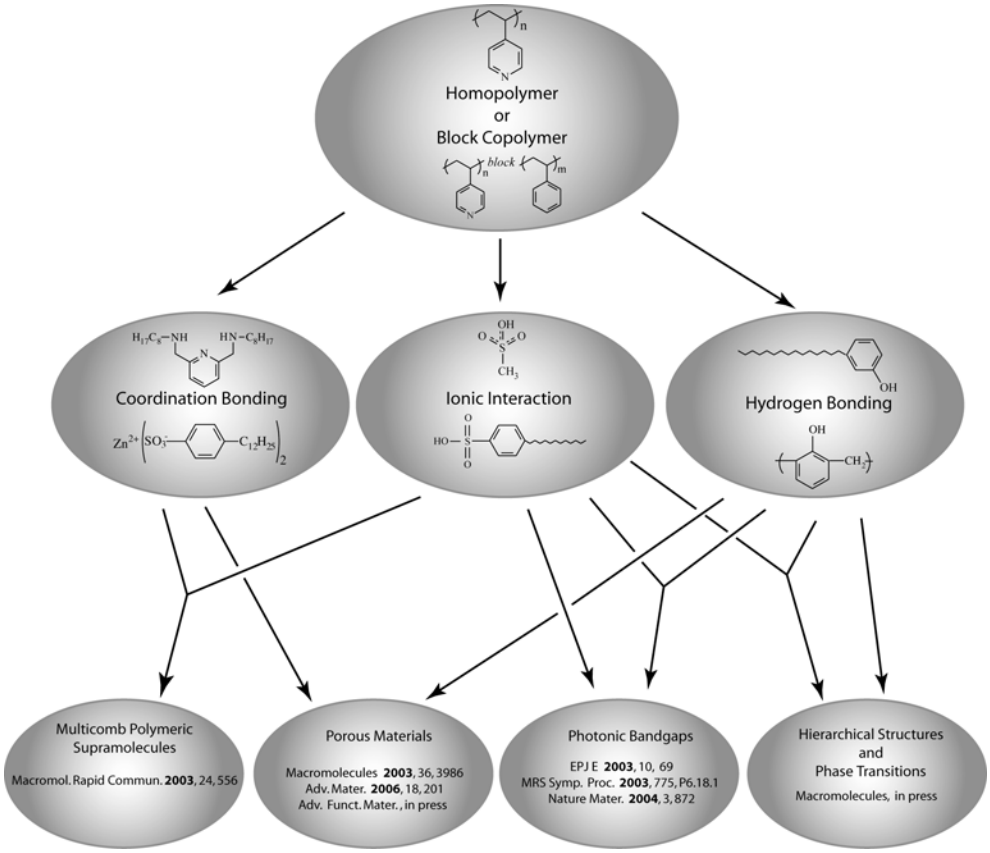

Figure 3. Schematics of the interactions used in this Thesis in order to prepare comb-shaped supramolecules and hierarchical self-assembly. These supramolecules can be used to obtain e.g. porous materials by cleaving the side chains or by controlled pyrolysis or photonic bandgap materials.

2. SELF-ASSEMBLED SUPRAMOLECULAR STRUCTURES AND PHASE TRANSITIONS

Different routes to tune the self-assembled structures of polymers have been described [22, 50, 75-78], where an important objective is to tune materials properties and functions to achieve functional materials. A rich variety of nanostructures has been obtained either using linear block copolymers [13, 16, 77] or covalently bonded dendritic side chains [78]. On the other hand, chemical moieties have been connected by hydrogen bonds or coordination to form polymer-like supramolecules [24, 48, 49, 56, 79-82]. In order to additionally achieve nanoscale structures by self-assembly, mutually repulsive moieties must be incorporated within the supramolecules [12, 25, 29, 53, 64, 83, 84]. This can lead to functional materials, as the structures, their phase transitions, and kinetics of the structure formation can be tailored [40, 50, 51, 85-87]. The comb-shaped architecture is particularly feasible as the physically bound "combs" also plasticize the structures, which leads to enhanced kinetics to promote well-developed order, which is especially useful for rigid polymers [86, 87] or for polymers of high molecular weight [88-90].

2.1. Hierarchical structures of comb-coil supramolecules and their phase transitions (Article I)

In Article I the hierarchical self-assembly and thermoreversible phase transitions of comb-coil supramolecules are studied for two systems consisting of hydrogen bonded side chains. In these systems polystyrene-*block*-poly(4-vinylpyridine) (PS-*block*-P4VP) diblock copolymer is either hydrogen bonded with 3-pentadecylphenol (PDP) (i.e. PS-*block*-P4VP(PDP)$_{1.0}$) or first protonated with methanesulfonic acid (MSA) and then hydrogen bonded to PDP (i.e. PS-*block*-P4VP(MSA)$_{1.0}$(PDP)$_{1.0}$). Previously these kind systems have been shown to be useful to achieve thermal switching of electrical and optical properties [51, 90].

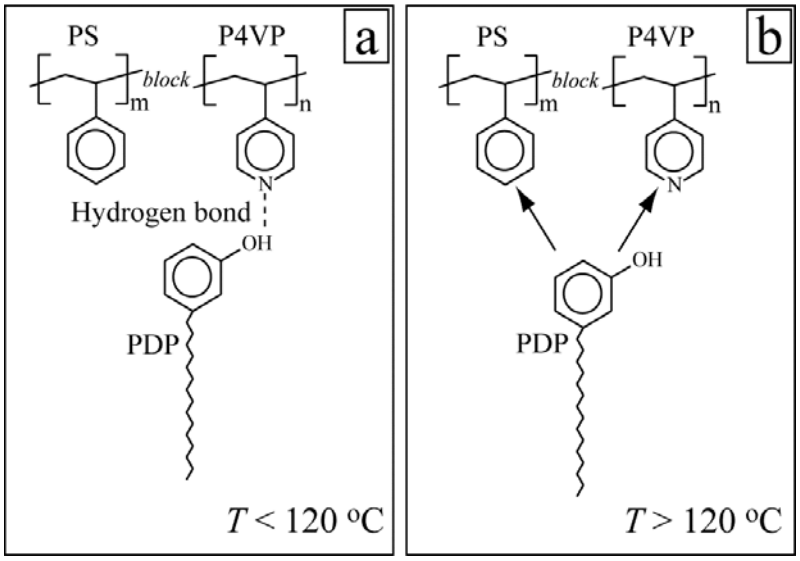

Figure 4. Schematics of the interactions in PS-*block*-P4VP(PDP)$_{1.0}$. **a)** At room temperature PDP is hydrogen bonded to P4VP and not soluble in PS. Upon heating the hydrogen bonds are gradually broken and **b)** at ca. T > 120°C PDP becomes also soluble in PS, i.e. it can diffuse into the PS domains.

Figure 4 illustrates the interactions PS-*block*-P4VP(PDP)$_{1.0}$ system: At room temperature PDP is hydrogen bonded to P4VP. Upon heating the hydrogen bonds are gradually broken and at ca. T > 120°C PDP becomes also soluble in PS, which enables diffusion of PDP molecules

into the PS domains leading to changes in volume fractions and concurrent order-order transitions. Figure 5 shows a representative example of the phase transitions upon heating:

1) Sample PS-*block*-P4VP(PDP)$_{1.0}$ with the P4VP(PDP)$_{1.0}$ weight fraction 0.62 contains at room temperature a gyroid-*in*-lamellar (GYR-*in*-*lam*) structural hierarchy, consisting of gyroidal block copolymer structure and smaller length scale lamellar structure within the P4VP(PDP)$_{1.0}$ matrix resulting from the lamellar self-assembly between the non-polar alkyl tails of PDP and the polar P4VP chains (Figure 5a).

2) The order-disorder transition (ODT) of the smaller structure occurs at ca. T = 60 °C and only the gyroid structure remains.

3) Upon further heating a lamellar structure is observed at T = 170 °C and hexagonally perforated layer (HPL) at T = 210 °C (Figure 5b and c).

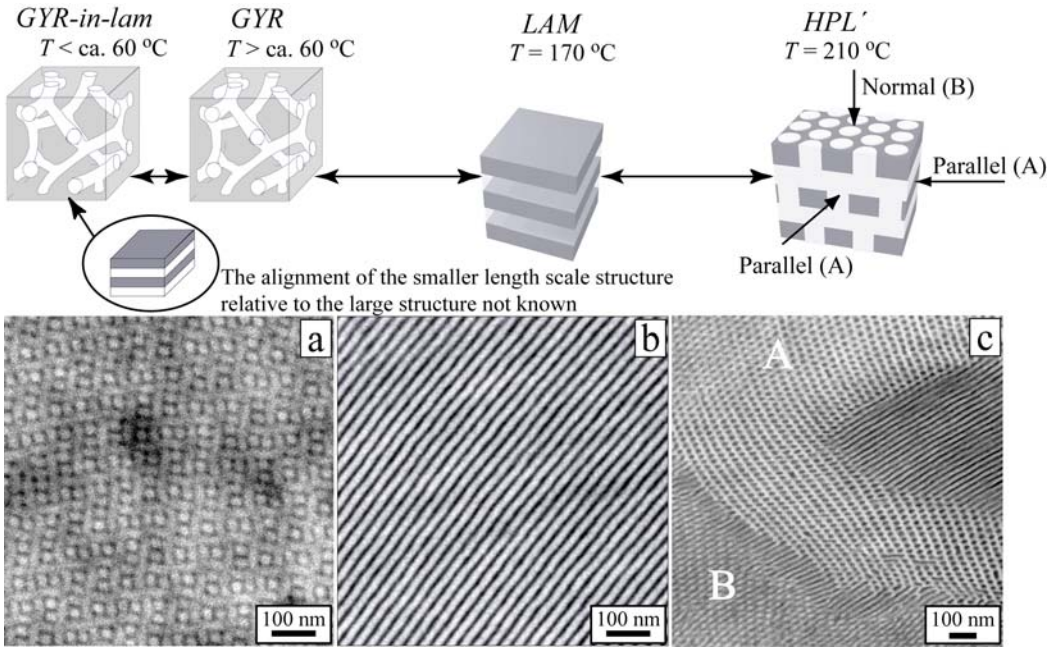

Figure 5. TEM micrographs of PS-*block*-P4VP(PDP)$_{1.0}$ with the P4VP(PDP)$_{1.0}$ weight fraction 0.62 ($M_{n,PS}$ = 31,900 g/mol, $M_{n,P4VP}$ = 13,200 g/mol). **a)** At room temperature a gyroid-*in*-lamellar structure is formed. At ca. T = 60 °C lamellar structure of P4VP(PDP)$_{1.0}$ undergoes an ODT and only the gyroid structure remains. **b)** At ca. T = 170 °C a lamellar structure and **c)** at ca. T = 210 °C a hexagonally perforated layer were observed. The normal and parallel projections of the HPL´ structure are illustrated in the scheme. The P4VP domains appear dark in the images due to the I_2 staining.

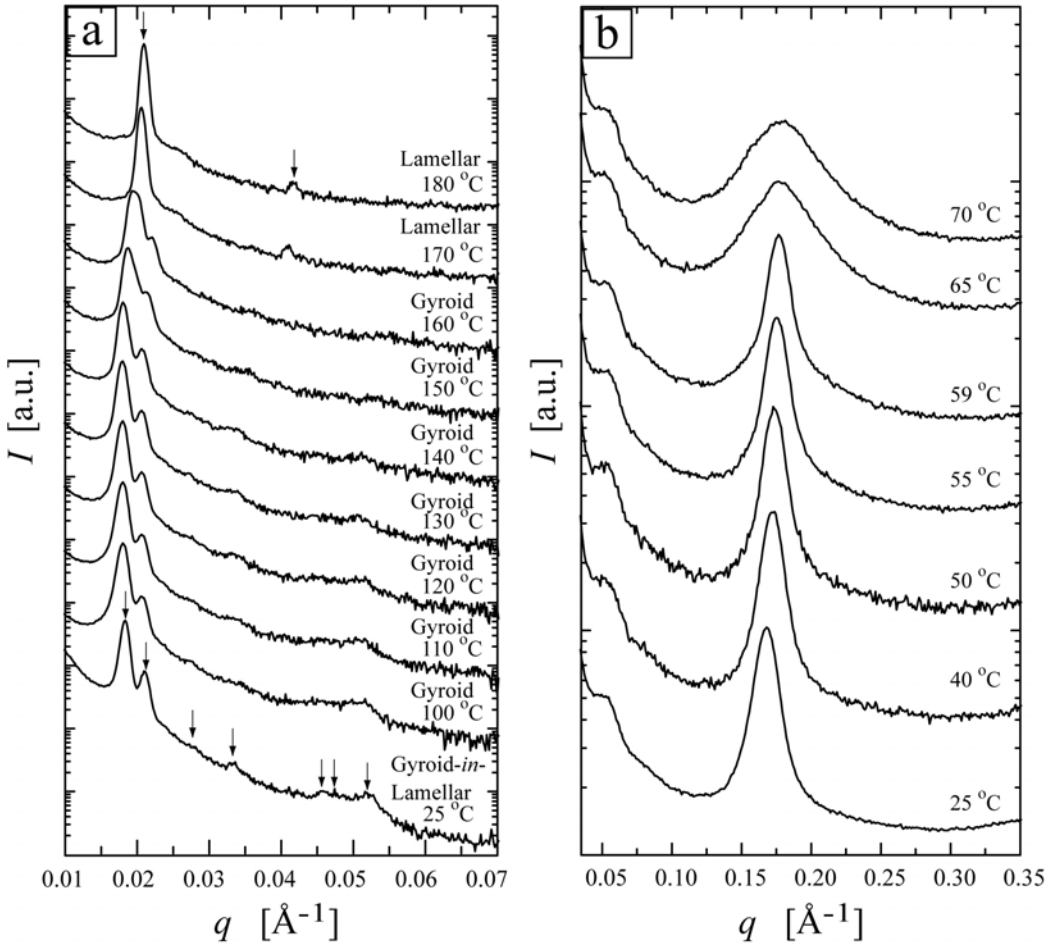

Figure 6. a) SAXS intensity patterns of PS-*block*-P4VP(PDP)$_{1.0}$ with the P4VP(PDP)$_{1.0}$ weight fraction 0.62 ($M_{n,PS}$ = 31,900 g/mol, $M_{n,P4VP}$ = 13,200 g/mol), as a function of temperature indicating a gyroid to lamellar transition at ca. T = 170 °C. **b)** The order-disorder transition of short length scale structure within P4VP(PDP)$_{1.0}$ domains occurs at ca. T = 60 °C, which can be seen as a broadening of the intensity maximum.

The phase transitions were also studied using small angle X-ray scattering (SAXS). Figures 6a and b show the SAXS intensity patterns at different temperatures indicating the gyroid-to-lamellar transition (Figure 6a) and ODT within the P4VP(PDP)$_{1.0}$ domains at ca. T = 60 °C (Figure 6b) upon heating. The determination of the exact temperatures of the phase transitions is still in progress.

Also several other order-order transitions were observed for the PS-*block*-P4VP(PDP)$_{1.0}$ system, such as lamellar-*in*-lamellar => lamellar => HPL or spherical-*in*-lamellar => cylindrical => HPL. A complete morphology diagram in heating is shown in Figure 7. All PS-*block*-P4VP(PDP)$_{1.0}$ samples showed at least two order-order transitions and some of them showed even four consecutive ordered phases.

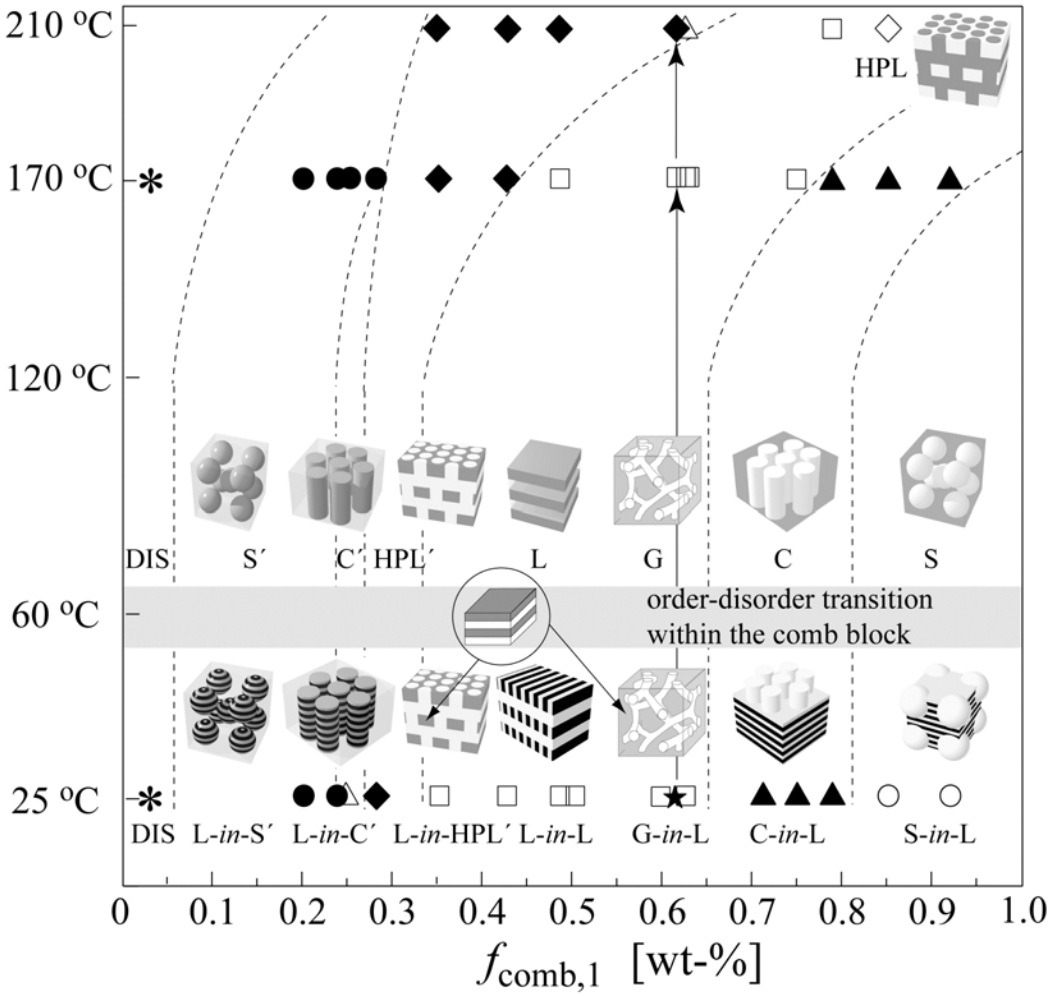

Figure 7. Morphology diagram for PS-*block*-P4VP(PDP)$_{1.0}$ upon heating as a function of the weight fraction of comblike block P4VP(PDP)$_{1.0}$ ($f_{comb,1}$). For lamellar-*in*-HPL´ and gyroid-*in*-lamellar morphologies the orientation of the smaller length scale structure within the P4VP(PDP)$_{1.0}$ domains is still unknown and therefore not drawn. The prime symbol (´) refers to phases where PS forms the matrix. Note that $f_{comb,1}$ is based on the nominal room temperature composition.

In the other system, i.e. PS-*block*-P4VP(MSA)$_{1.0}$(PDP)$_{1.0}$, diblock copolymer is first protonated with methanesulphonic acid (MSA) and then hydrogen bonded to PDP. In this system the phase behavior is more complex owing to the additional phase separation of PDP at ca. T = 175 °C from the P4VP(MSA)$_{1.0}$ domain into the PS domain [51], causing substantial increase in volume fraction of PS domain (Figure 8). Furthermore, the ODT of the smaller length scale structure within the P4VP(MSA)$_{1.0}$(PDP)$_{1.0}$ domains occurs at higher temperature than for PS-*block*-P4VP(PDP)$_{1.0}$ system at T = 125 °C.

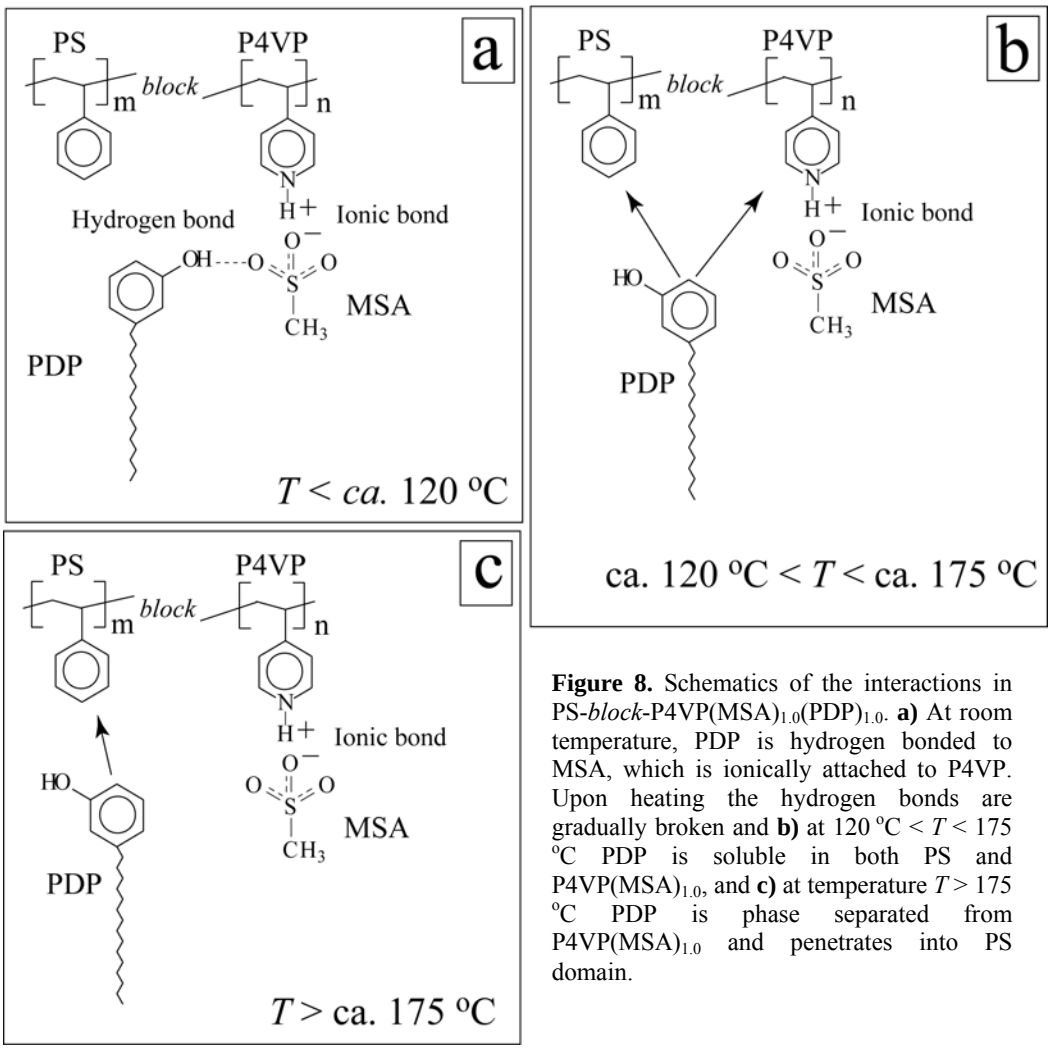

Figure 8. Schematics of the interactions in PS-*block*-P4VP(MSA)$_{1.0}$(PDP)$_{1.0}$. **a)** At room temperature, PDP is hydrogen bonded to MSA, which is ionically attached to P4VP. Upon heating the hydrogen bonds are gradually broken and **b)** at 120 °C < T < 175 °C PDP is soluble in both PS and P4VP(MSA)$_{1.0}$, and **c)** at temperature T > 175 °C PDP is phase separated from P4VP(MSA)$_{1.0}$ and penetrates into PS domain.

The observed order-order transitions upon heating for this system are collected in Figure 9. In some samples even five consecutive phase transitions are observed, e.g. lamellar-*in*-lamellar => lamellar => HPL => cylindrical => spherical structure. As PDP is phase separated from the P4VP(MSA)$_{1.0}$ domains into PS domains, only spherical structures were observed at T > 175 °C. The order-order transitions in these materials are based on the changes in volume fractions, which enable to obtain reversible transition sequences that are not possible only by changing the Flory-Huggins interaction parameter χ by temperature, e.g. from lamellar to spherical structure.

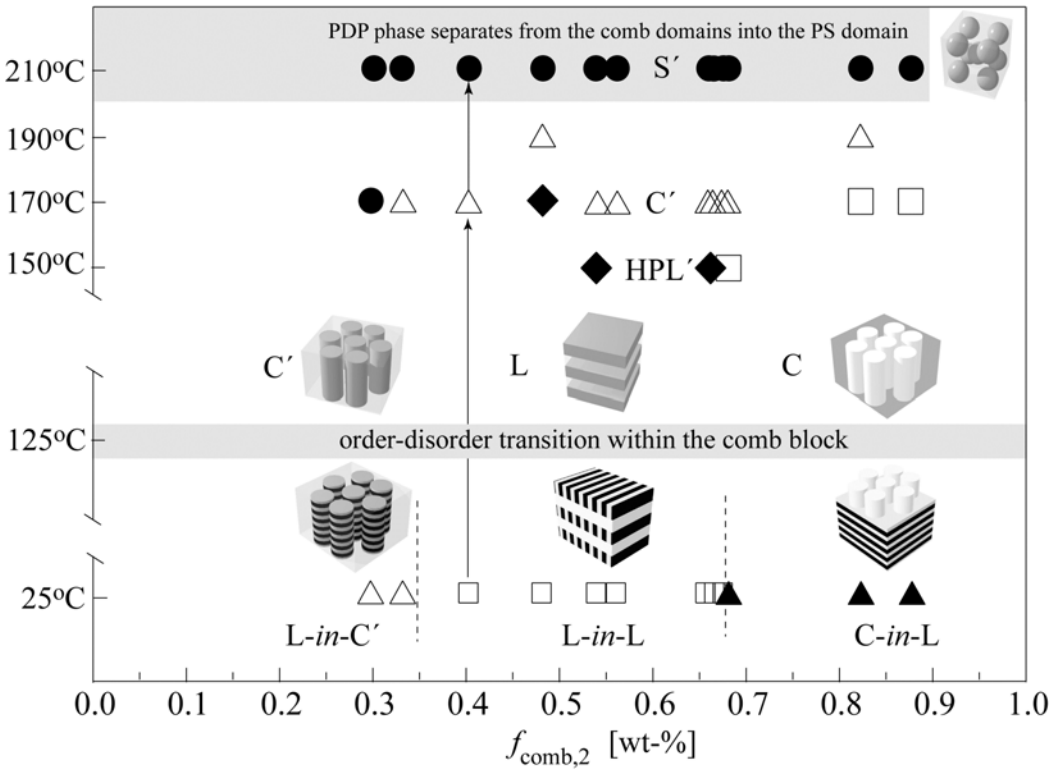

Figure 9. Morphology diagram of PS-*block*-P4VP(MSA)$_{1.0}$(PDP)$_{1.0}$ upon heating as a function of weight fraction of the comb block ($f_{comb,2}$) at different temperatures. The prime symbol (´) refers to phases where PS is matrix. Note that $f_{comb,2}$ is based on the room temperature compositions.

2.2. Multicomb polymeric supramolecules (Article II)

Article I described how self-assembled structures can be controlled using hydrogen bonded side chains. In Article II we used a combination of different physical interaction, i.e. coordination and ionic interaction, to attach several alkyl chains to one repeat unit. This system is denoted as multicomb polymeric supramolecules, as there is a particularly dense set of side chains vs. each polymer repeat unit. Compared to dendron-modified polymers [78], where the synthesis can be challenging, this approach allows a facile concept to control the side chain crowding by attaching several side chains vs. each repeat unit of the polymer backbone. This enables a rational tailoring of the self-assembled structures as the length and number of the side chains is easily tunable.

The multicomb polymeric supramolecules consist of poly(4-vinylpyridine) (P4VP), whose pyridine groups have been Zn(II)-coordinated to 2,6-bis-(*n*-octylaminomethyl)-pyridine bearing two octyl side chains. Importantly, the two dodecylbenzenesulfonate counter-ions also contain alkyl tails providing an enhanced side chain crowding (Figure 10).

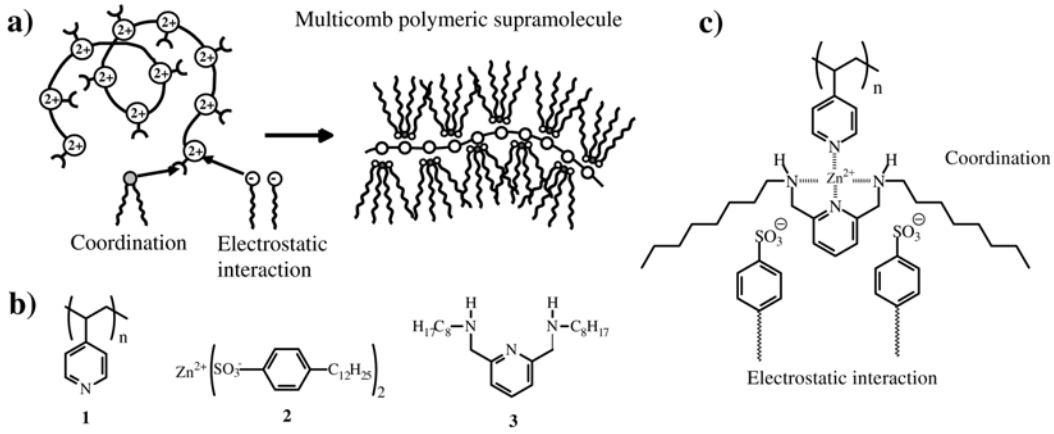

Figure 10. a) A concept to bond several side chains vs. one repeat unit of the polymer backbone based on coordinated alkylated ligands and alkyl-functionalized counter-ions. **b)** The starting materials: P4VP (**1**), $Zn(DBS)_2$ (**2**), and 2,6-bis-(*n*-octylaminomethyl)-pyridine (**3**). **c)** The suggested complexation within the 1:1:1 molar mixture of P4VP, $Zn(DBS)_2$, and 2,6-bis-(*n*-octylaminomethyl)-pyridine to form polymeric supramolecules poly[(4VP)Zn(2,6-bis-(*n*-octylaminomethyl)-pyridine)$(DBS)_2$].

The formation of supramolecular entities was studied using Fourier Transformation Infrared spectroscopy (FTIR). Figures 11a and b represent FTIR data of the relevant bands near 1600 cm^{-1} and 1000 cm^{-1}, respectively. Bands of 2,6-bis-(*n*-octylaminomethyl)-pyridine at 1592 cm^{-1} and 1577 cm^{-1} (curve 2) assigned to the uncomplexed nitrogens are observed to shift to higher wavenumbers (1606 cm^{-1} and 1585 cm^{-1}, respectively) upon complexation with Zn^{2+} (curve 3). In the tricomponent mixtures of P4VP, 2,6-bis-(*n*-octylaminomethyl)-pyridine, and $Zn(DBS)_2$ a new absorption band shoulder (label I) is formed at about 1620 cm^{-1} (curves 4 and 5). Previously similar shifts have been observed when P4VP participates coordination bonding [44-46, 91]. Another evidence is provided by the reduced absorption at 993 cm^{-1} of pyridines upon complexation (label II) [44]. Based on FTIR spectroscopy as well as quantum chemical calculations using density functional theory, and sample homogeneity in optical microscopy, formation of supramolecular entities represented in Figure 10c is suggested. In these supramolecules the ligand, 2,6-bis(octylaminomethyl)pyridine, is attached to the P4VP via zinc coordination and also the DBS^- counterions are now used as structure forming motifs (Note that counter-ions of the coordinated supramolecules are usually not paid much attention).

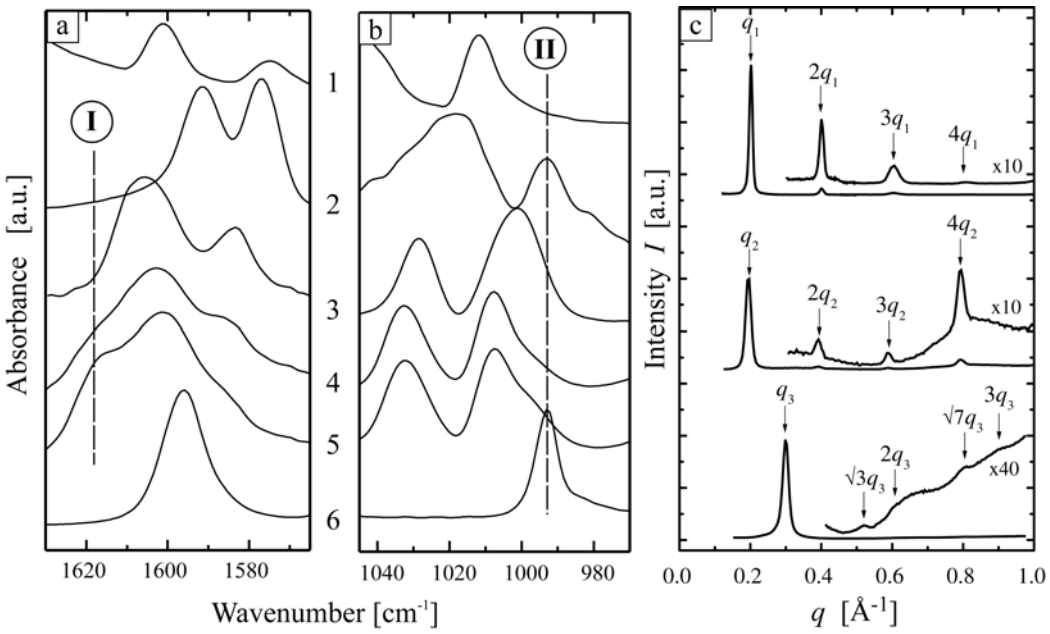

Figure 11. a) FTIR absorption spectra for 1) $Zn(DBS)_2$, 2) 2,6-bis-(*n*-octylaminomethyl)-pyridine, 3) mixture of 2,6-bis-(*n*-octylaminomethyl)-pyridine and $Zn(DBS)_2$ (molar ratio 1:1), 4) 1:1:1 molar mixtures of P4VP, $Zn(DBS)_2$, and 2,6-bis-(*n*-octylaminomethyl)-pyridine, 5) 1:0.5:0.5 molar mixtures of P4VP, $Zn(DBS)_2$, and 2,6-bis-(*n*-octylaminomethyl)-pyridine, and 6) P4VP. Label I indicates the expected shoulder at ca. 1620 cm^{-1} due to coordination of the pyridine moieties in the vicinity of the phenyl group absorption (ca. 1600 cm^{-1}). **b)** Label II indicates the absorption at 993 cm^{-1} of the uncomplexed pyridines that become shifted upon complexation. **c)** SAXS intensity curves for $Zn(DBS)_2$ (uppermost curve), 2,6-bis-(*n*-octylaminomethyl)-pyridine (curve in the middle), and 1:1:1 mol mixture of P4VP, $Zn(DBS)_2$, and 2,6-bis-(*n*-octylaminomethyl)-pyridine (undermost curve). The latter shows narrow peaks with several higher orders, suggesting hexagonal order.

Morphology of the multicomb polymeric supramolecules was characterized using SAXS (Figure 11c) and grazing incidence diffraction experiments (GIXD) (Figure 12). Both $Zn(DBS)_2$ and 2,6-bis-(*n*-octylaminomethyl)-pyridine formed a lamellar structure with a long period of about L_p = 3.1 nm (two uppermost curves in Figure 11c). The amorphous P4VP, in turn, shows no peaks. However, the mixture of P4VP, $Zn(DBS)_2$ and 2,6-bis-(*n*-octylaminomethyl)-pyridine in the molar ratio 1:1:1 shows a particularly narrow and high-intensity first order maximum at q_3 = 0.30 $Å^{-1}$ and higher order reflections at $\sqrt{3}q_3$, $2q_3$, $\sqrt{7}q_3$, and $3q_3$ (the bottom curve in Figure 11c), corresponding to cylindrical self-assembly in the tricomponent mixture. Hexagonal order was also confirmed from films using GIXD (Figure 12), where the material was sheared at elevated temperature (ca. T = 150 °C) by drawing a microscope cover slip on a Si-substrate. Three discrete intensity maxima are observed at q_3 = 0.30 $Å^{-1}$ indicating a six-fold symmetry.

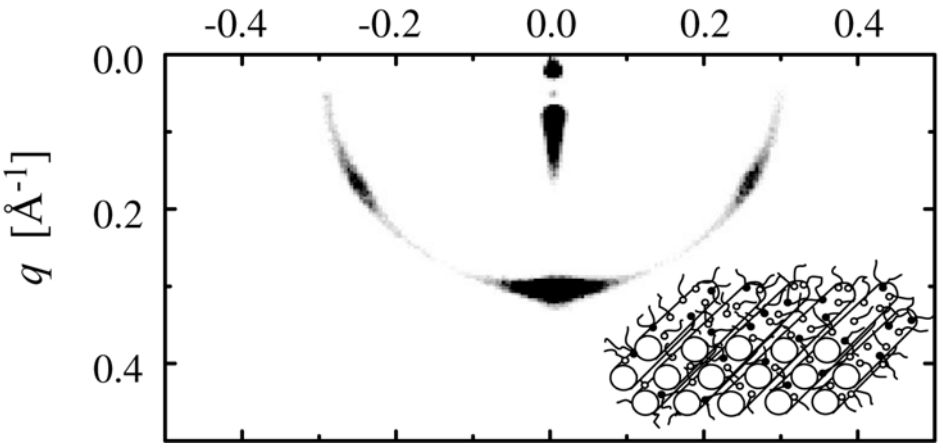

Figure 12. GIXD intensity pattern for poly[(4VP)Zn(2,6-bis-(*n*-octylaminomethyl)-pyridine)$(DBS)_2$] showing a hexagonal structure in films that have been oriented by drawing a microscope cover slip on a Si-substrate. The inset shows a possible scheme of self-assembly.

3. PHOTONIC BANDGAP MATERIALS BASED ON COMB-COIL SUPRAMOLECULES

The self-assembly and phase behavior of comb-shaped supramolecules were studied in Articles I-II. The comb-shaped architecture leads to stretching of chains and the amphiphilic side chains act as platizicers providing better local structures even with high molecular weight samples. In Articles III-V we demonstrate that these concepts can be used to prepare photonic bandgap materials and may even lead to switching properties.

3.1. Photonic bandgap materials

The detailed manipulation of the flow of light has become of great interest in the fields of optical communication, optical computation, sensing, optical limiting and coatings [92-101]. Photonic crystals are defined as ordered structures with a periodic variation the dielectric constant [95]. The photonic bandgap, i.e., the range of frequencies in which the propagation of the photons is prohibited, is determined by the periodicity, dimensionality, and dielectric contrast of the crystal [95]. Combined with controlled defect structures, a wealth of applications in photonics is expected: e.g. capability to trap, guide and control light.

A variety of methods to construct photonic bandgap materials have been demonstrated. Lithographic, etching, and holographic techniques enable the preparation of detailed structures and defects with sufficient dielectric contrast [102-107]. These *top-down* approaches typically require many processing steps and for certain large area applications *bottom-up* techniques could be more proper. On the other hand, spontaneous self-assembly of colloids [108], synthetic opals [109-116], inverted opals [111, 117-119], and block copolymers [73, 88-90, 101, 106, 120-131] allows preparation of small enough structures based on competing interactions. Although self-assembly leads to a well-defined local order and offers a potentially low-cost method for the production of photonic crystals, it is challenging to achieve perfectly ordered structures over the macroscopic length scale combined with carefully engineered defects and large enough dielectric contrast.

Block copolymers form a variety of self-assembled 1D, 2D, and 3D periodic structures and thus provide a platform for preparation of photonic crystals. However, it is challenging to achieve structures with well-defined macroscopic order approaching the optical wavelength $\lambda/2n$, where λ is the wavelength and n is the refractive index, as high molecular weight polymers would be needed, which leads to very slow relaxations and poor long-range order. This has been overcome by swelling the block copolymer domains with narrow molecular weight homopolymers, oligomeric plasticizers, physically bonded amphiphiles or liquid crystals [73, 88-90, 120-123, 132] (Figure 13). Another challenge is the inherently low dielectric contrast in most organic polymers (refractive index typically ca. 1.5). In order to increase the dielectric contrast, high-refractive index nanoparticles, such as Au, CdSe, and SiO_2, have been selectively incorporated to the structures [120, 122, 133-135] (Figure 13).

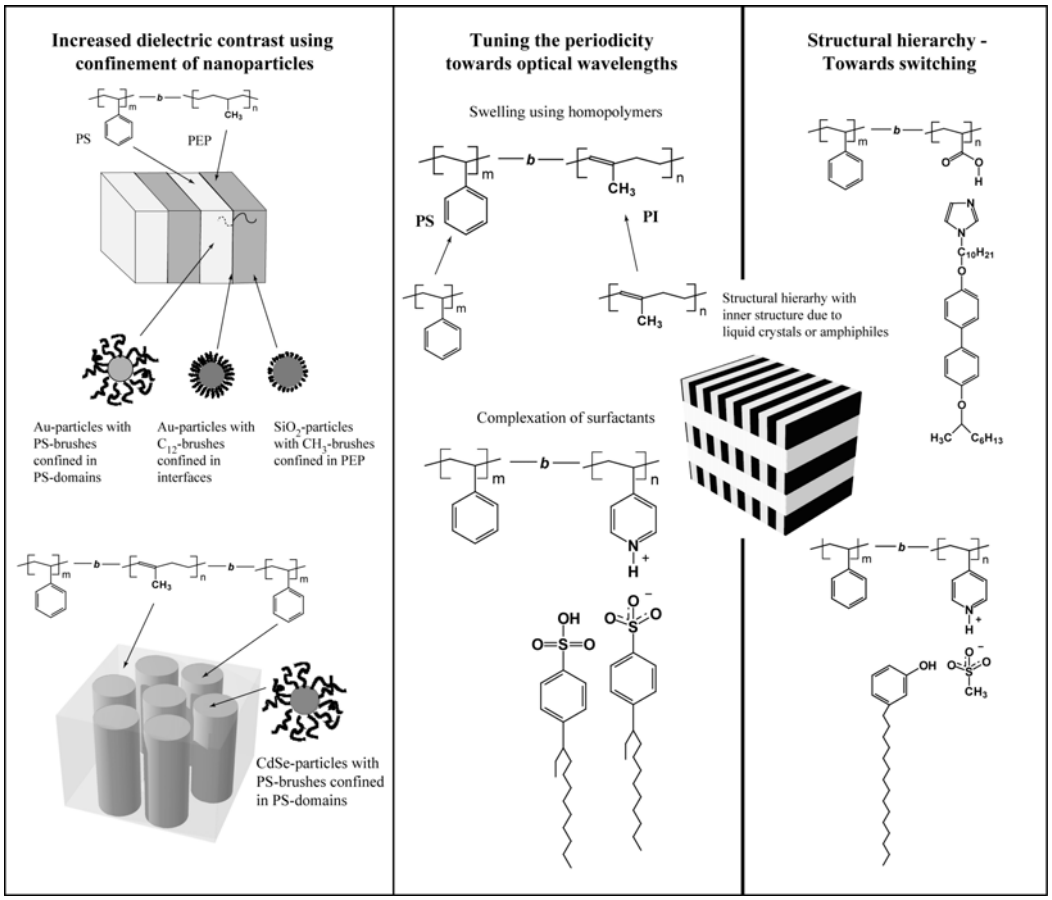

Figure 13. Examples of block copolymeric systems towards photonic bandgap materials [73, 88-90, 120-123, 132-135].

Recently, concepts for switching bandgaps have been demonstrated based on, e.g., liquid crystals [73, 136], hydrogels and colloids [109, 137-139], mechanical tuning of plastic opals [115], and thermochromism [113]. Block copolymer based photonic bandgap materials, in which the optical properties can be tuned or switched by applying various external fields, have also been constructed. Thermally switchable photonic bandgap materials have been prepared using comb-coil supramolecules, where the switching results from the changes in either refractive index [73] or the periodicity of the system [90]. The periodicity of the system can also be tuned by applying mechanical force, which has been demonstrated using block copolymeric gels [101, 115].

3.2. One-dimensional photonic bandgap (Articles III – IV)

In Articles III and IV we demonstrate that one-dimensional optical reflectors can be prepared using high molecular weight diblock copolymer PS-*block*-P4VP ($M_{n,PS}$ = 238 100 g mol^{-1} and $M_{n,P4VP}$ = 49 500 g mol^{-1}) and dodecylbenzenesulfonic acid (DBSA). DBSA side chains are bonded to the pyridines by protonation and hydrogen bonding leading to comb-coil supramolecules PS-*block*-P4VP(DBSA)$_y$, where y denotes the degree of complexation (Figure 14a). They self-assemble in a hierarchical manner, where the larger structure corresponds to the block copolymer structure and the smaller length scale structure within the comb block (P4VP(DBSA)$_y$) results from the self-assembly between the polar polymer backbone and alkyl tails of the DBSA molecules (Figure 14b). The structures were investigated using SAXS and TEM revealing a lamellar structure with a long period in excess of 100 nm (Figure 14c). The particularly large lamellar periodicity results from the comb-shaped architecture, which causes a considerable stretching of the polymer chains and allows long periods sufficient to serve as a one-dimensional optical reflector. In addition, DBSA molecules plasticize the material enabling better structure formation even without annealing or macroscopic alignment.

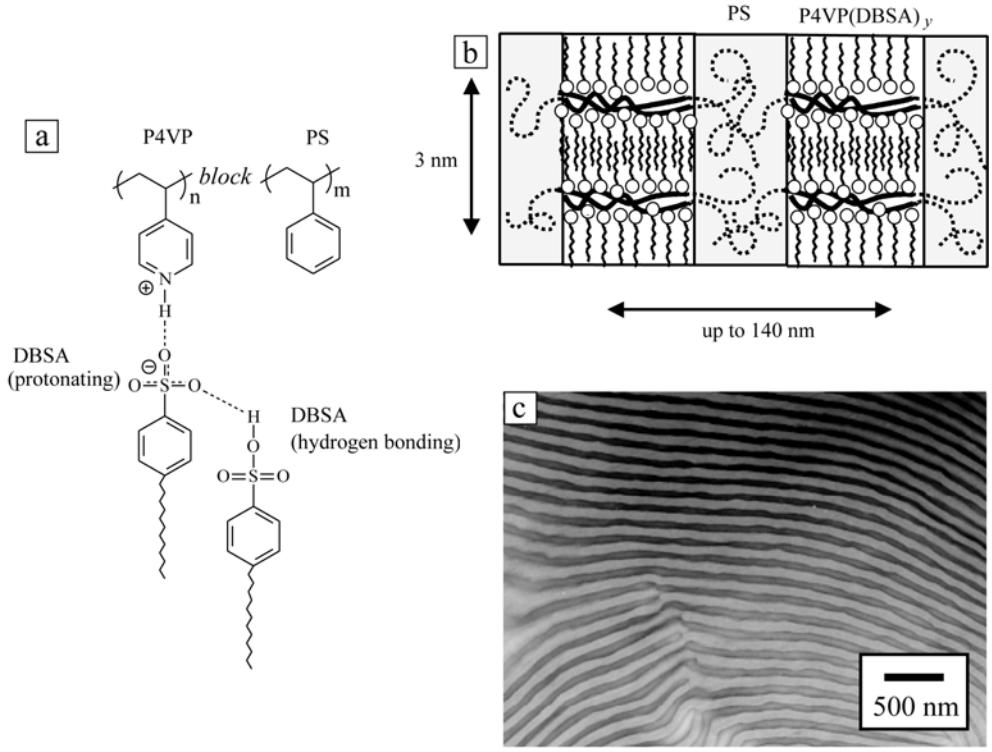

Figure 14. a) The proposed scheme for the bonding between PS-*block*-P4VP and DBSA and **b)** structural hierarchy. Note that part of the DBSA molecules can be hydrogen bonded to P4VP instead of protonation. **c)** TEM micrograph of high molecular weight complex PS-*block*-P4VP(DBSA)$_{2.0}$ illustrating the lamellar structure with a long period ca. 140 nm. The P4VP(DBSA)$_{2.0}$ phase shows dark in the image due to I_2 staining. Thicknesses of PS and P4VP(DBSA)$_{2.0}$ lamellae are almost equal, which qualitatively agrees with the P4VP(DBSA)$_{2.0}$ weight fraction w = 0.60.

Figure 15 shows the transmittance and reflectance curves in the visible wavelength range for complexes PS-*block*-P4VP(DBSA)$_y$. Sample PS-*block*-P4VP(DBSA)$_{1.0}$ starts to show reduced transmission at ca. 400 nm and sample with y = 1.5 has an incomplete and fairly narrow bandgap at ca. 460 nm (the relative width of the reflectivity peak, $\Delta\lambda/\lambda$, is ca. 0.20). Also PS-

block-P4VP(DBSA)$_{2.0}$ shows a slightly broader bandgap (Figure 15a). The position of the mid-gaps qualitatively agrees with the long period of sample ($\lambda/2n$ condition) based on TEM and X-ray scattering studies. Typically the refractive index n of these kinds of polymers is of the order 1.5 – 1.6, which partly explains the narrowness and incompleteness of gap. Figure 15b shows the reflectance measurements for the complexes confirming the formation of photonic bandgap. The reflectance peaks were observed at 370 nm, 460 nm, and 470 nm for complexes y = 1.0, 1.5, and 2.0, respectively. The samples were predominantly blue pearlescent (Figure 15c), as represented in the photographs of the complexes with different degree of complexation y.

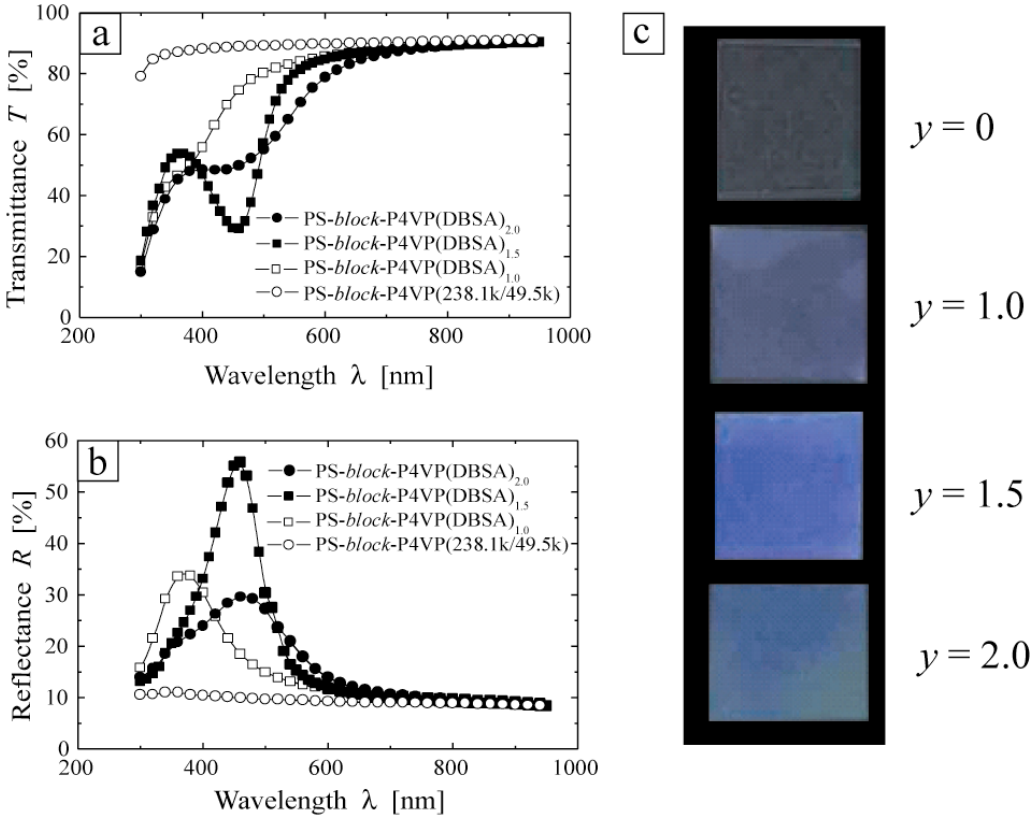

Figure 15. UV-Vis **a)** specular transmission and **b)** diffuse reflectance measurements for complexes PS-*block*-P4VP(DBSA)$_y$ indicating the formation of bandgap at ca. 370 – 470 nm. **c)** Photograph of the samples with different degree of complexation y.

Owing to the lamellar one-dimensional structure, also the angular dependence of the mid-gap position was studied for PS-*block*-P4VP(DBSA)$_{1.5}$ by tilting different angles (θ) from the normal to the sample (Figure 16). The bandgap was blue-shifted to ca. 400 nm when the angle increased from 0° to 60° (Figure 16a). The position of the mid-gap with different incident angles of the light is plotted in the Figure 16b (black squares). The solid line in Figure 16b illustrates calculated mid-gap position for an ideal multi-layer stack with average refractive index n = 1.6 and it coincides well with the measured values.

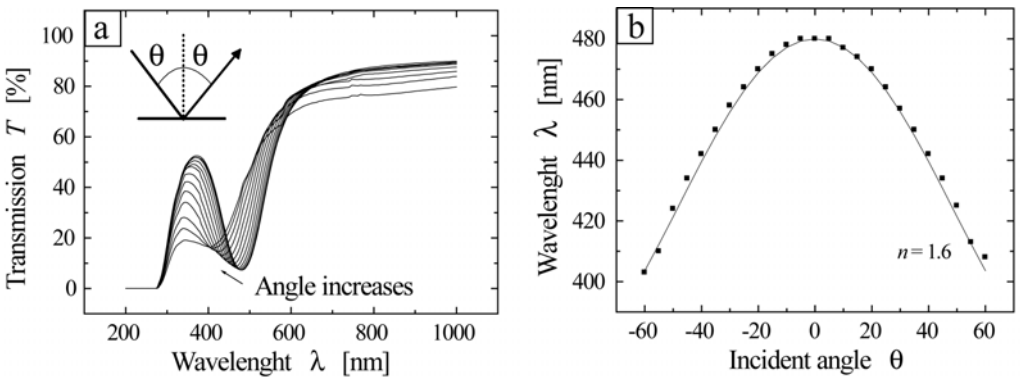

Figure 16. a) UV-Vis transmission graphs for PS-*block*-P4VP(DBSA)$_{1.5}$ with different incident angles of the light ($\theta = 0 - 60^{o}$). **b)** A plot of the mid-gap position vs. the incident angle of the light (black squares). Calculated mid-gap position for an ideal multi-layer stack structure with different incident angle is drawn as a solid line (the average refractive index is approximated to be $n = 1.6$).

3.3. Temperature induced reversible photonic bandgap switching (Article V)

The photonic bandgaps demonstrated in Articles III-IV did not show optically responsive or switching behaviour. In Article V, the additional temperature responsivity is gained by bonding alkyl combs (PDP) by weaker hydrogen bonding instead of strong ionic interaction, still keeping the protonation of P4VP(MSA)$_{1.0}$ leading to supramolecules PS-*block*-P4VP(MSA)$_{1.0}$(PDP)$_{1.5}$ (Figure 17a). The phase behaviour of the system was studied in Article I, but now the molecular weight of the diblock copolymer is considerable higher in order to obtain sufficient long periods required for photonic bandgap materials in the visible wavelength range. The interaction between PS-*block*-P4VP and MSA was studied using FTIR spectroscopy. Figure 17b shows FTIR absorption bands for MSA, PDP, and PS-*block*-P4VP as well as for the complex PS-*block*-P4VP(MSA)$_{1.0}$(PDP)$_{1.5}$ at different temperatures. Due to the protonation the stretching band of pyridine ring is shifted from 1597 cm^{-1} to 1637 cm^{-1} confirming the protonation of P4VP [8]. The intensity of the absorption band of the protonated pyridine does not remarkable change as a function of temperature indicating that MSA molecules are attached to P4VP. Hydrogen bonding between P4VP(MSA)$_{1.0}$ and PDP was, however, more difficult to deduce and the solubility changes between P4VP(MSA)$_{1.0}$/PDP and PS/PDP, which were observed with optical microscope [51], could not be resolved with FTIR.

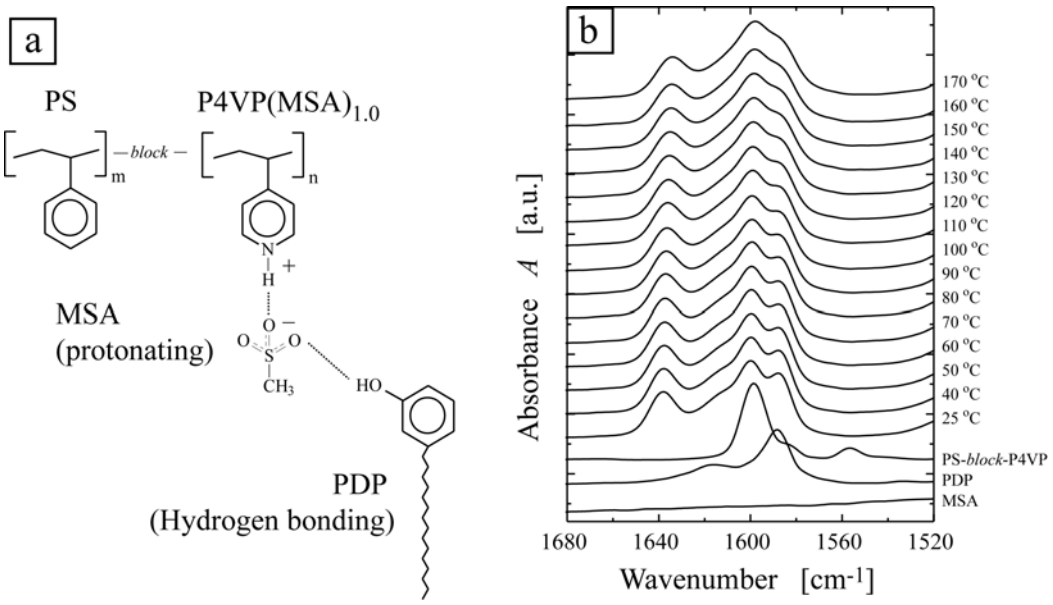

Figure 17. a) Schematics for the interactions of PS-*block*-P4VP(MSA)$_{1.0}$(PDP)$_{1.5}$ at room temperature. **b)** FTIR spectra for MSA, PDP, and pure PS-*block*-P4VP at room temperature and for the complex PS-*block*-P4VP(MSA)$_{1.0}$(PDP)$_{1.5}$ as a function of temperature indicating a protonation between pyridine and MSA.

The structure of the complex PS-*block*-P4VP(MSA)$_{1.0}$(PDP)$_{1.5}$ was examined using TEM (Figure 18c and f) and SAXS (Figure 19). Figure 18c shows a lamellar self-assembled structure having a long period of ca. 160 nm and the sample is green in reflection (Figure 18b). Below T = 130 °C, the periodicity was larger than the available q-range of the synchrotron SAXS and no intensity maxima were observed (Figure 19a). Faint indication of the first intensity maximum starts to appear at ca. T = 130 °C and the sample turns uncolored (Figure 18e). Five equally spaced intensity maxima are observed at T = 170 °C, indicating a lamellar structure with a long period of ca. 117 nm. Figure 19b shows reversibility of the

lamellar long period as a function of temperature. The lamellar structure at high temperature was confirmed by quenching the sample from T = 170 °C to liquid propane, and the TEM micrograph showed lamellar structure (Figure 18f).

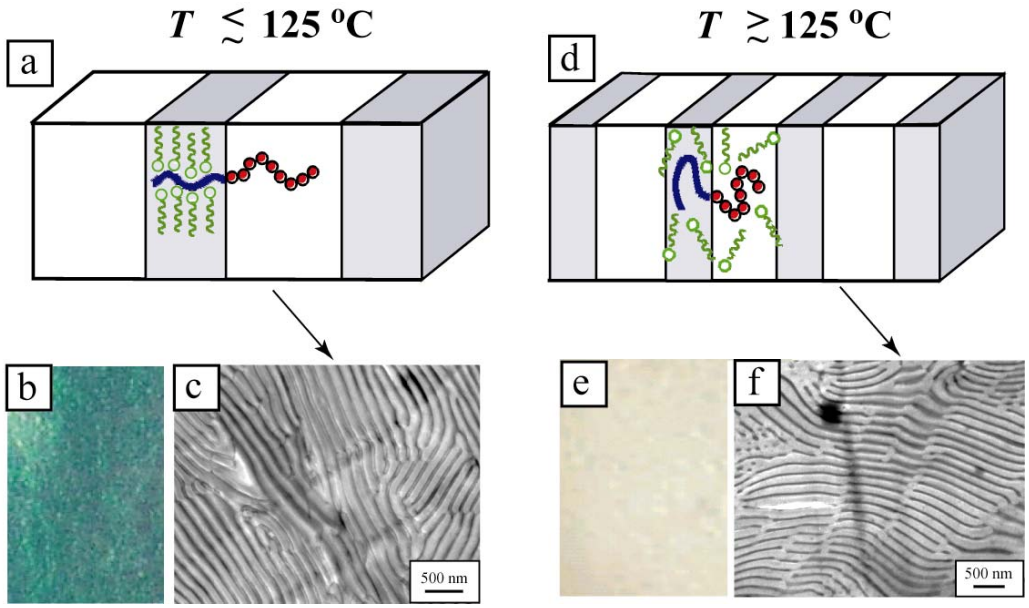

Figure 18. Schematics for PS-*block*-P4VP(MSA)$_{1.0}$(PDP)$_{1.5}$ at room temperature and at $T \geq 125$ °C: **a)** At room temperature PDP is a selective solvent for the P4VP(MSA)$_{1.0}$ and the sample has structural hierarchy. **b)** At room temperature the sample is green. **c)** The TEM shows the lamellar structure, with the long period of ca. 160 nm due to stretching of the chains. The smaller structure is not resolved. **d)** At $T \geq 125$ °C, PDP becomes a non-specific solvent for PS and P4VP(MSA)$_{1.0}$ and there is no internal structure within the P4VP(MSA)$_{1.0}$-containing domains. **e)** At $T \geq 125$ °C the sample is uncolored. **f)** Rapid quenching of the sample from T = 170 °C shows a lamellar structure, as confirmed by SAXS.

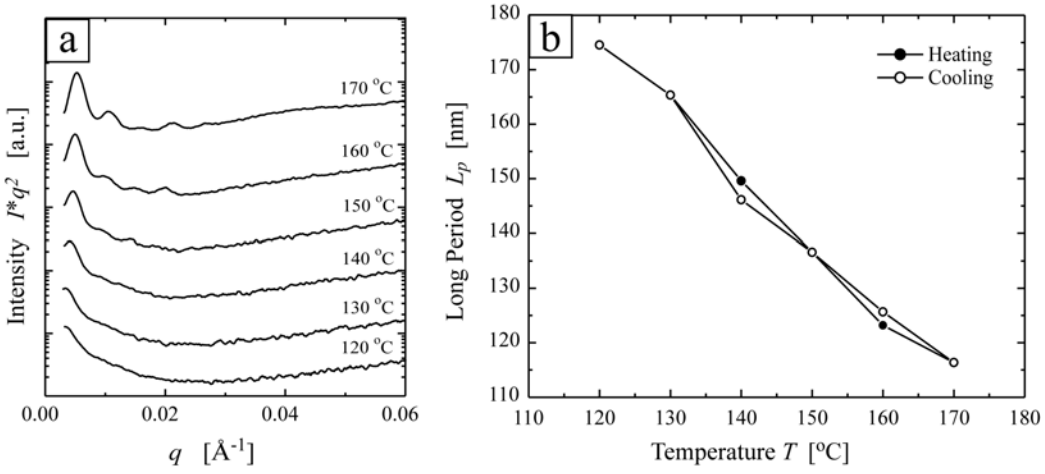

Figure 19. a) SAXS curves of PS-*block*-P4VP(MSA)$_{1.0}$(PDP)$_{1.5}$ at different temperatures. **b)** The long period of the lamellar structure as a function of temperature.

At low temperatures material contains a smaller structure within P4VP(MSA)$_{1.0}$(PDP)$_{1.5}$ domains, i.e., structure-*within*-structure hierarchy (Figure 18a) [72]. The smaller structure has an order-disorder transition (ODT) at ca. T = 125 °C, which can be seen as a stepwise broadening of the SAXS reflection at q = 0.147 Å^{-1} (corresponding to a long period of 4.3

nm). This was also observed as a sudden change in the square of half-width half-maximum, $(\text{h.w.h.m.})^2$ as a function of 1000/T (K^{-1}) (Figure 20A; inset) and as a disappearance of the birefringent texture in optical microscope on passing $T = 125^{o}C$ [90].

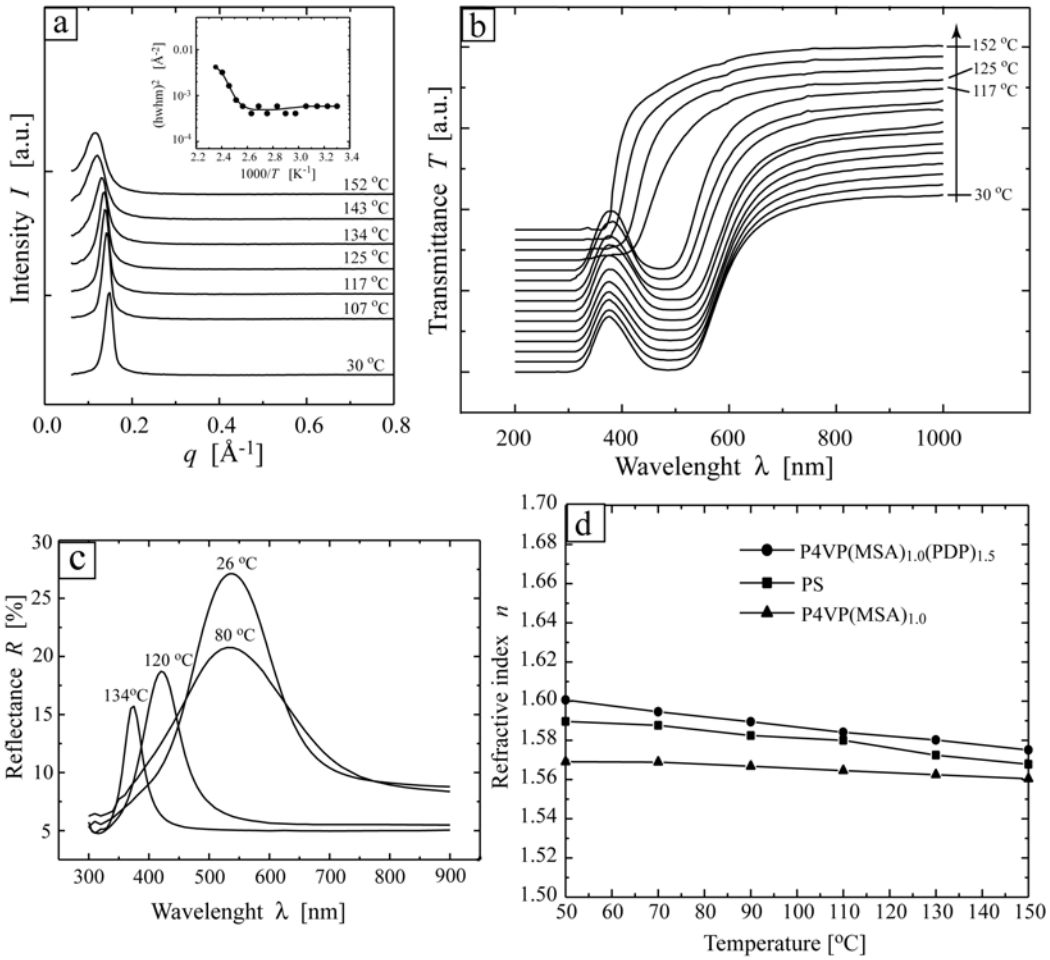

Figure 20. a) The order-disorder transition within the P4VP(MSA)$_{1.0}$(PDP)$_{1.5}$ -domains is observed at ca. 125 °C seen as a broadening of the peak and as a sudden change in the square of half-width at half-maximum, $(\text{h.w.h.m.})^2$, as a function of 1000/T (K^{-1}), as represented in the inset. **b)** UV-Vis transmission measurements of PS-*block*-P4VP(MSA)$_{1.0}$(PDP)$_{1.5}$: Upon heating the position of the bandgap remains same up to ~ 117 °C. Further increase in temperature caused a large change of the position of the bandgap to the smaller wavelengths (> 100 nm) in very narrow temperature range. **c)** Similar response was observed in the reflectance measurements, where peaks were located at 530 nm, 530 nm, 420 nm, and 370 nm corresponding temperatures 26 °C, 80 °C, 120 °C, and 134 °C, respectively. **d)** Refractive indexes of PS, P4VP(MSA)$_{1.0}$, and P4VP(MSA)$_{1.0}$(PDP)$_{1.5}$ as a function of temperature.

Optical properties were determined using UV-Vis transmission and reflection measurements as a function of temperature (Figures 20b and c). At room temperature, UV-Vis transmission curve indicates a bandgap located at ca. 500 nm. Upon heating, the position of the bandgap remained approximately constant up to ca. $T = 117$ °C and further heating caused a large shift (> 100 nm) of the bandgap position to smaller wavelengths within a narrow temperature range (< 15 °C). The switching of the bandgap position was confirmed with reflection measurements (Figure 20c). Increasing the temperature from room temperature to ca. 80 °C decreases the intensity of reflection, while the position remained at ca. 530 nm. Further increase of temperature shifts the peak position to 420 nm and 370 nm corresponding to 120

°C and 134 °C, respectively. This was manifested as a major change in colour of the sample from green to uncoloured (Figure 18b and e).

The mechanism behind the switching behaviour is the same as in Article I and our previous studies [51]: On heating hydrogen bonds between PDP and P4VP(MSA)$_{1.0}$ are gradually broken and at ca. T = 120 – 130 °C PDP becomes soluble in PS. This induces a very strong decrease in the long period of the lamellar structure within a narrow temperature range, as the comb-shaped supramolecular architecture of the P4VP(MSA)$_{1.0}$ chains is lost, thus allowing more compact coiling of the polymer.

As the changes in the refractive indexes may also influence to the switching behaviour, their temperature dependence was studied using ellipsometry. Figure 20d represents the refractive indexes of PS, P4VP(MSA)$_{1.0}$, and P4VP(MSA)$_{1.0}$(PDP)$_{1.5}$ separately as a function of temperature. They changed smoothly only few percents when heated up to ca. T = 140 °C suggesting that optical switching is due to the changes in the lamellar periodicity. Furthermore, as the order-disorder transition of the smaller structure within P4VP(MSA)$_{1.0}$(PDP)$_{1.5}$ domains occurred close to the photonic bandgap switching temperature for PS-*block*-P4VP(MSA)$_{1.0}$(PDP)$_{1.5}$, we wanted to study whether the order-disorder transition of the smaller structure is coupled to the bandgap switching. The order-disorder transition temperature of the smaller structure can be tailored by changing the concentration of PDP. Figure 21b shows the UV-Vis transmission spectra for PS-*block*-P4VP(MSA)$_{1.0}$(PDP)$_{2.0}$ showing a similar photonic bandgap switching at ca. T = 125 °C but where the order-disorder transition occurs at ca. T = 60 °C (Figure 21a) clearly excluding the role of ODT in the switching.

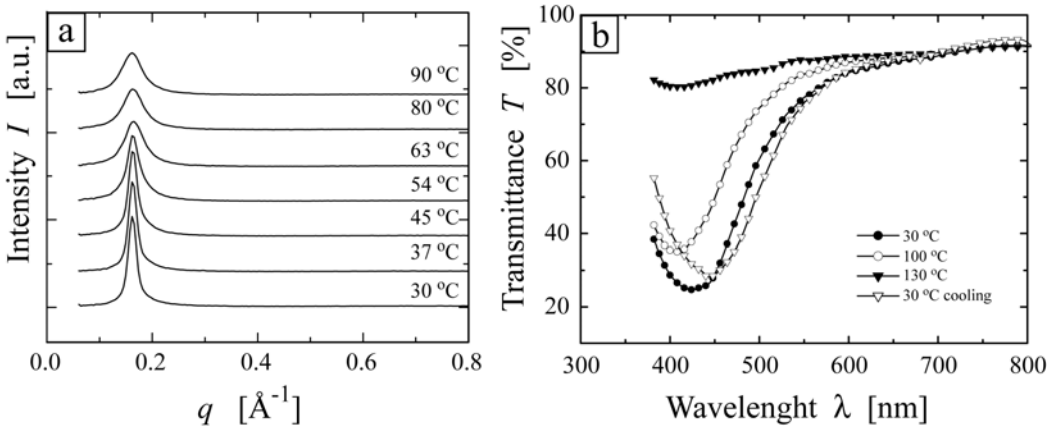

Figure 21 a) The order-disorder transition within the P4VP(MSA)$_{1.0}$(PDP)$_{2.0}$ -domains is observed at ca. 60 °C. **b)** UV-Vis transmission measurements of PS-*block*-P4VP(MSA)$_{1.0}$(PDP)$_{2.0}$ representing a photonic bandgap switching at ca. T = 125 °C.

In addition, several attempts to tune the switching temperature using different sulfonic acids instead of MSA has been investigated; such as *p*-toluene sulfonic acid (TSA), dodecylbenzene sulfonic acid (DBSA), chiral and rasemic camphor sulfonic acids (+/-/±)CSA, and dinonylnaftalene sulfonic acid (DNNSA). They did not, however, show switching effects as a function of temperature owing to the stronger interaction, possibly due to an additional phenyl ring stacking between PDP and the acid, prohibiting the migration of PDP into PS domains [140] [141].

4. TEMPLATE ASSISTED APPROACHES FOR FUNCTIONAL POROUS MATERIALS

The self-assembly and phase behavior of comb-shaped supramolecules were studied in Articles I-II and preparation of photonic bandgap materials in Articles III-V. In photonic bandgap materials the use of physical interactions instead of covalent ones allowed switching effects. Physical interactions also enable the cleavage of entities once the structure is formed, leading to e.g. porous materials. In this chapter the results of the Articles VI-VIII are presented, where we describe two template-assisted approaches towards functional porous materials, i.e., selective extraction of coordinated amphiphiles and controlled pyrolysis of block copolymer in the presence of phenolic resin.

4.1. Porous materials

Biological systems provide several examples for porous materials, where a high density of pores with regular sizes and proper biochemical functionality lead to selectivity and functionality. Also synthetic functional membranes have major technological applications, e.g. in sensors, separation materials, filters, templates for catalysis, biomaterial engineering, electronics and optoelectronics [142-145]. Several concepts to prepare porous materials ranging from micro- or nanoporous (pores < 2 nm), mesoporous (< 50 nm) up to macroporous (> 50 nm) have been previously demonstrated [6, 9, 45, 47, 85, 112, 146-176]. The nanoporous materials are typically crystalline framework solids, such as zeolites, discotic molecular assemblies [147, 148, 161], or "robust" molecular crystals formed using supramolecular [24] design principles [83, 146, 150, 152, 154, 162, 168-170, 172, 177]. These materials can have large void volumes and high internal surface areas, but the supramolecular materials often tend to collapse upon emptying the pores. Several approaches have also been presented to prepare mesoporous and macroporous materials, such as "track-etching" [6, 159, 163], using honeycomb structures [153, 158, 175], and emptying nanostructured templates (e.g., sol–gel processing of surfactants or block copolymers [151, 157, 160, 165], selective degradation of material with UV exposure [149, 174, 176], pyrolysis [155, 156, 171, 173, 178, 179], chemical etching [180-183], and selective removal of low molecular- weight amphiphiles (combs) from hierarchically self-assembled polymeric comb–coil supramolecules [45, 85]).

For optimal transport of fluids and gases, hierarchical porous materials are required, i.e. materials with pores on different length scales. Compared to the monomodal porous materials, hierarchical porous materials typically have enhanced properties due to increased mass transport through the material (macropores > 50 nm) combined with higher surface area facilitating higher activities and better-controlled selectivities (micropores < 2 nm and mesopores 2 - 50 nm) [184] like in e.g. bones, lungs, and wood. Several concepts to prepare hierarchical bi- or trimodal porous materials have been reported, including e.g. micro-macroporous [185], micro-mesoporous [186, 187], meso-macroporous [188-192], bimodal mesoporous [193, 194], bimodal mesoporous–macroporous [195] and micro-meso-macroporous materials [196-198].

Among the various concepts for creating porous materials, the template-assisted approach provides a facile way to obtain well-defined structures on different length scale, a wide range of pore sizes, and chemical functionalities [9, 143, 191, 199, 200]. Examples of suitable structure-directing agents include molecular species [191, 199], surfactants or block copolymers [45, 85, 149, 151, 157, 160, 165, 174, 176, 178, 179], colloids [201, 202], emulsions [203], polymer gels [204], vesicles [205], foams [190, 206], solid particles, and bacteria [207]. By combining different structure-directing agents, the structures can be controlled over a hierarchy of different independent length scales in the same material. Block copolymers, in turn, provide ideal structures for templates, as they self-assemble into various

structures as a result of the repulsion between covalently bonded blocks; such as spherical, cylindrical, lamellar, and gyroid structures[13, 17, 76]. The advantage of polymers compared to e.g. molecular crystal based porous materials is that they can "lock" the porosity preventing structure from collapsing. In addition, polymers allow tunability in functionality and in pore size over a wide range.

4.2. Removal of coordinated amphiphiles by extraction with selective solvent (Article VI)

As already mentioned above, physical interactions enable the cleavage of entities once the structure is formed, leading to porous materials. Previously this concept has been demonstrated in hydrogen bonded comb-coil supramolecules in preparation of "hairy tubes"[85]. In Article VI we used stronger physical interaction between the amphiphiles and diblock polymer (coordination bonding), which allows using of higher molecular weight amphiphiles and offers a wider variety of amphiphiles (see e.g. Article II). This, in turn, could lead to higher porosity after selective removal of amphiphiles.

Accordingly, we used a coordination complex consisting of zinc dodecylbenzenesulfonic acid [$Zn(DBS)_2$] and PS-*block*-P4VP diblock copolymer (Figure 22a) and in order to demonstrate concepts for pores of different sizes, different molecular weights were used. The complex formation was confirmed using FTIR spectroscopy, which showed a shifted pyridine absorption at 1619 cm^{-1} corresponding to the complex formation between Zn^{2+} and P4VP [43, 44, 46] (Figure 22b). The self-assembled structures were characterized using SAXS and TEM and they formed a lamellar-*in*-lamellar self-assembly, where the smaller structure within P4VP[$Zn(DBS)_2$]$_y$ domains is formed by alternating polar polymer backbone and non-polar dodecyl alkyl chains (Figure 22a). As no efforts were made to align the lamellar structures, they do not have a common orientation and a relatively large number of defects were observed.

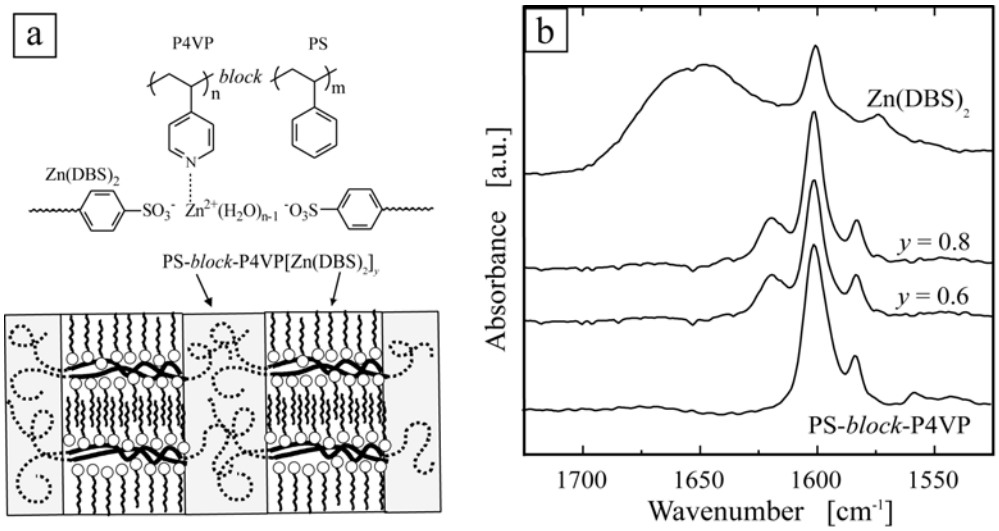

Figure 22. a) Schematic picture of the proposed coordination bonding between PS-*block*-P4VP and $Zn(DBS)_2$ and lamellar-*in*-lamellar structure of PS-*block*-P4VP[$Zn(DBS)_2$]$_{0.9}$. **b)** FTIR absorption bands for $Zn(DBS)_2$, PS-*block*-P4VP[$Zn(DBS)_2$]$_y$, and PS-*block*-P4VP. The formation of coordination bond is seen as a shift of the aromatic carbon-nitrogen stretching band from 1597 cm^{-1} to ca. 1619 cm^{-1} when the pyridine group participates in metal-ligand π-bonding.

After structure formation, the amphiphiles were removed from the hierarchical structure by extracting with methanol, which is a selective solvent for P4VP and $Zn(DBS)_2$. Figure 23a

represents the SAXS intensity patterns before (dots) and after (solid line) extraction. Due to the removal of $Zn(DBS)_2$ the intensity maximum corresponding to the internal structure within the $P4VP[Zn(DBS)_2]_y$ domain (ca. q = 0.20 Å^{-1}) is disappeared. In addition, the long period was not affected by the methanol extraction and the higher order peaks corresponding to the block copolymer structure are resolved more clearly in the extracted sample, possibly due to the enhanced electron scattering density difference. The inset illustrates that the data is fitted remarkably well with the ideal lamellar model as given by the solid curve. The removal of $Zn(DBS)_2$ was also observed as a contrast inversion between stained and unstained samples in TEM (Figure 23c and d). These results show that despite the relatively open lamellar structure, the glassy PS domains, the different orientations of the nonaligned lamellae, and the relatively high number of defects stabilize the structure and prevent it from collapsing, leaving at least partially open pores.

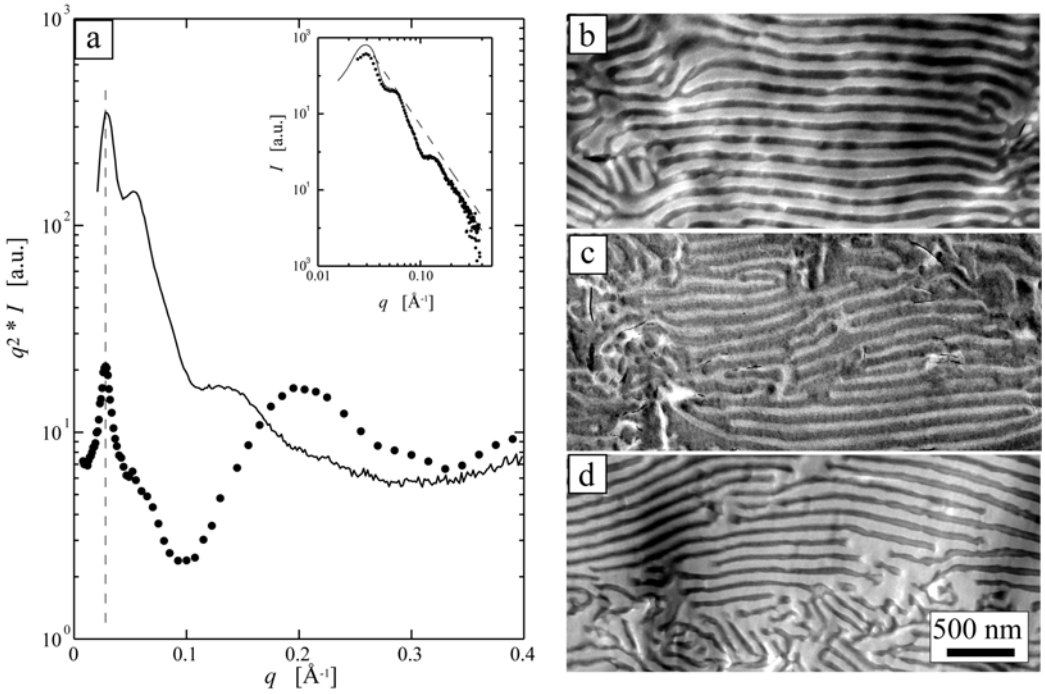

Figure 23. a) SAXS intensity patterns for PS-*block*-$P4VP[Zn(DBS)_2]_{0.60}$ before (dots) and after (solid line) $Zn(DBS)_2$ removal ($M_{n,PS}$ = 41,400 g/mol, $M_{n,P4VP}$ = 1,900 g/mol). The inset illustrates that the data is fitted remarkably well with the ideal lamellar model as given by the solid curve. This model features infinite parallel lamellae with a long period of ca. 210 Å. **b)** TEM-micrograph for PS-*block*-$P4VP[Zn(DBS)_2]_{0.9}$ showing a lamellar structure. The $P4VP[Zn(DBS_2)]_{0.9}$ domain shows dark due to the I_2 staining. **c)** The lamellar structure for the methanol extracted and unstained sample, where the electron deficient P4VP/air domain is now white. **d)** The extracted and I_2 stained sample where the P4VP domain shows dark due to the increased electron density in that domain. It should be noted that if the amphiphiles were not removed the $P4VP[Zn(DBS_2)]_{0.9}$ domain would always be dark in the images, with or without staining. ($M_{n,PS}$ = 238,100 g/mol, $M_{n,P4VP}$ = 49,500 g/mol).

4.3. Mesoporous phenolic resin by pyrolysis of block copolymer template (Article VII)

Article VI described a method to construct mesoporous materials using extraction with selective solvent. In Articles VII and VIII we demonstrate another concept to prepare porous materials using self-assembled thermosets. Self-assembled thermosets have been prepared e.g. by curing thermoset precursors[4] in the presence of block copolymers [208-220] or by polymerization of specific surfactant assemblies [221-225]. Furthermore, self-assembled structures have been demonstrated by polymerizing phenolic resin monomers in the presence of cationic surfactants [226] and block copolymers [227, 228].

Phenols form relatively strong hydrogen bonds with pyridines [229]. In Article VII the self-assembled thermosets are prepared using phenolic resin and PS-*block*-P4VP diblock copolymer complexes (Figure 24a). Owing to the hydrogen bonding between the pyridine and phenolic resin [218], self-assembled structures consisting of PS and P4VP/phenolic resin domains are formed (Figure 24b). The relative weight fractions of the domains are selected to obtain different morphologies, such as spherical, cylindrical, and lamellar. After structure formation the block copolymeric templates are degraded by controlled pyrolysis at T = 420 °C leading to mesoporous materials (Figure 24c).

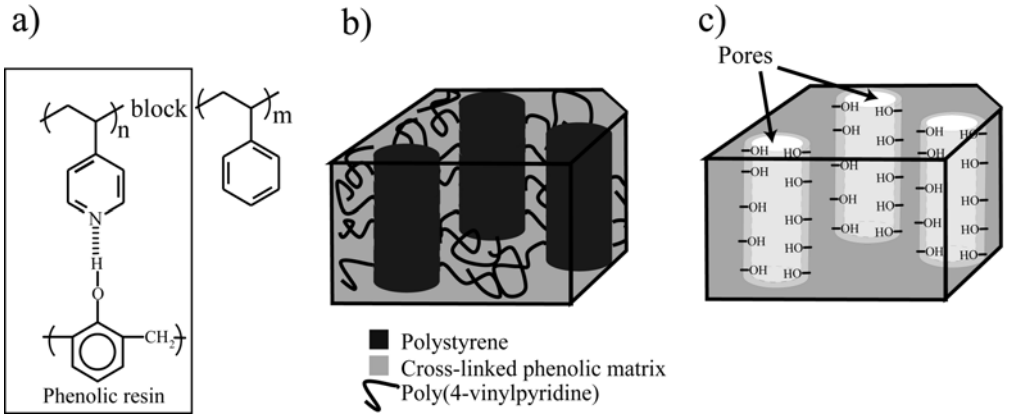

Figure 24. a) Phenolic resin, PS-*block*-P4VP and schematics of their mutual hydrogen bonding. **b)** Due to hydrogen bonding, the phenolic resin and P4VP are confined within the same self-assembled domains as they microphase separate from the nonpolar PS domains. Cross-linking at elevated temperatures "locks" the structure. **c**) During the selected pyrolysis conditions, PS-*block*-P4VP is essentially removed, leaving porous material with a narrow distribution of pore sizes, high surface area per volume unit, and hydroxyl groups at the porous matrix and the pore walls.

The porous structures were characterized using FTIR spectroscopy, TEM, SAXS, and UV-Vis spectroscopy. Figure 25a shows the FTIR spectra for the cylindrical structure (PS weight fraction in the complex w_{PS} = 40 %) before and after pyrolysis as well as for the reference samples. Pure PS-*block*-P4VP (curve 5) did not show absorption bands above 3200 cm^{-1}, whereas all samples containing phenols had a peak at 3430 cm^{-1} and a shoulder at ca. 3500 cm^{-1} corresponding to hydrogen-bonded and free phenolic OH-groups, respectively. This indicates that significant number of the hydroxyl groups remain after pyrolysis. The TEM image of the well-defined cylindrical porous structure is shown in Figure 25b.

[4] Precursors are typically low molecular weight (M_n ~ 500 – 5000 $gmol^{-1}$) epoxy or phenolic resins.

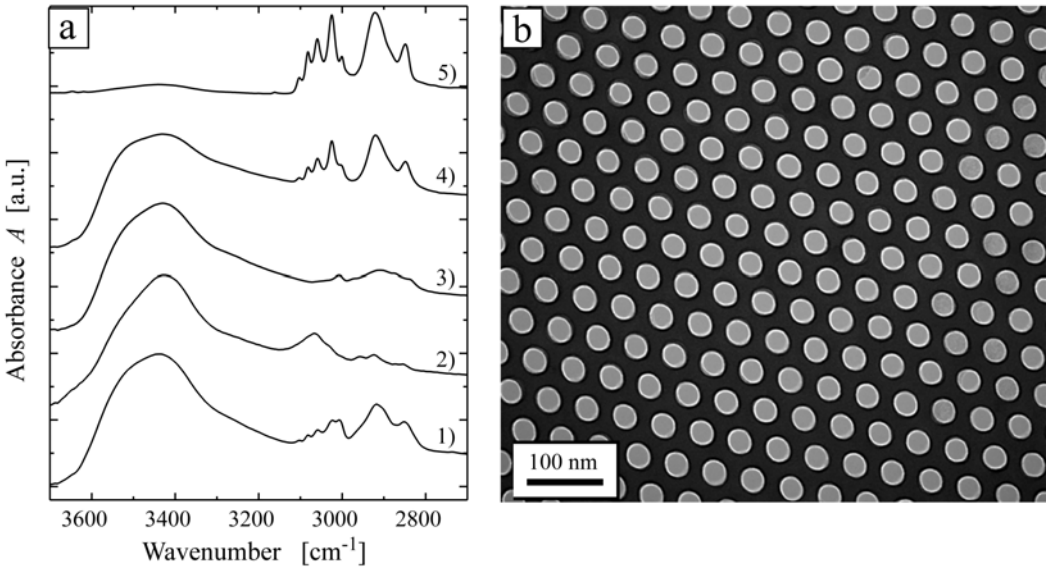

Figure 25. a) FTIR absorption bands in the range from 2700 cm^{-1} to 3700 cm^{-1} for the HMTA-cured PS-*block*-P4VP/phenolic resin complexes and PS-*block*-P4VP before and after pyrolysis. Samples are as follows; 1) w_{PS} = 0 % after pyrolysis, 2) w_{PS} = 40 % after pyrolysis, 3) w_{PS} = 0 % before pyrolysis, 4) w_{PS} = 40 % before pyrolysis, and 5) pure PS-*block*-P4VP. **b)** TEM image of w_{PS} = 40 % after pyrolysis showing a well-defined cylindrical structure.

The porous structure and hydroxyl groups at the matrix and pore walls (Figure 25a) are expected to lead to faster absorption rate and chemical selectivity. This was analysed using two different dye model compounds, i.e., Methylene blue hydrate (MB) and Rhodamine 6G (R-6G). MB is expected to have a stronger selective interaction owing to its nitrogen containing aromatic ring. Figures 26a and b show the UV-Vis absorbance as a function of time for cylindrical porous structure (Figure 25b) as well as for a reference sample (nonporous sample, i.e. pyrolyzed phenolic resin with w_{PS} = 0 %) immersed in dye solutions. The nonporous reference sample (w_{PS} = 0 %) hardly absorbs dye from the solution whereas the cylindrical porous sample (w_{PS} = 40 %) absorbs much more rapidly and the absorbance approaches zero after ca. 400 hours, indicating that most of the MB molecules have been absorbed from the solution (Figure 26a). In contrast, in the case of R-6G, which is expected to have weaker interaction, the absorbance for cylindrical porous sample (w_{PS} = 40 %) is leveled off to relatively high absorbance level, showing that a substantial amount of R-6G molecules still remains in the solution (Figure 26b). These results clearly support the expectations that the high absorption of MB molecules in the porous phenolic material results from the creation of porosity (as comparing the cases w_{PS} = 0 % *vs.* 40 % for MB) and that the hydrogen bonding between the dye molecules and phenolic OH-groups also plays an important role in absorption (as comparing the cases between MB and R-6G). Figure 26c shows the images of the MB solutions (Figure 26a) after ca. 1000 hours for sample w_{PS} = 40 % (transparent) and w_{PS} = 0 % (blue) illustrating the complete absorption of the dye molecules from the solution for the cylindrical porous w_{PS} = 40 % sample.

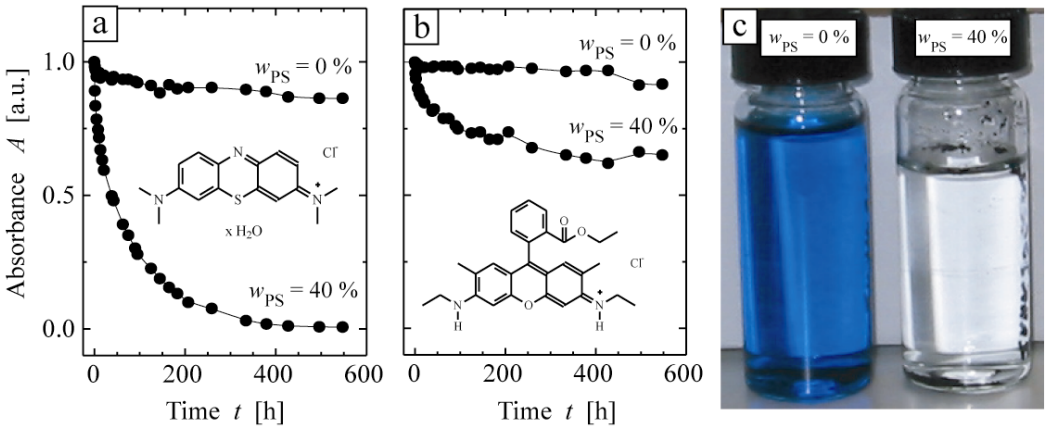

Figure 26. Methylene Blue hydrate (MB) and Rhodamine 6G (R-6G) concentrations in aqueous solutions as a function of time after addition of phenolic absorbents in the solutions. **a)** Concentration of MB based on its characteristic UV-Vis absorption at λ = 665 nm as a function of time. **b)** Concentration of R-6G based on its characteristic UV-Vis absorption at λ = 277 nm as a function of time. Note that the absorbance depends on the concentration logarithmically. **c)** Images of the MB solutions (Figure 26a) after ca. 1000 hours for w_{PS} = 0 % and w_{PS} = 40 % illustrating the complete absorption of the dye molecules from the solution for the porous w_{PS} = 40 % sample.

4.4. Hierarchical porous materials (Article VIII)

The aim of Article VIII was to prepare hierarchical porous materials and tune the porosity simply by controlling the post process conditions. Based on our previous results, the weight fractions of PS-*block*-P4VP and phenolic resin were selected to obtain cylindrical structure, i.e., w_{PS} = 40 % (Figure 27a and b). The block copolymer template was selectively removed by varying pyrolysis conditions. Moderate pyrolysis conditions lead to monomodal mesoporous materials, as essentially only the PS block is removed, whereas during prolonged isothermal pyrolysis at T = 420 °C also the P4VP block is removed leading to hierarchical micro-mesoporous structures (Figure 27c). In addition, the controlled pyrolysis leaves phenolic hydroxyl groups at the pore walls, and matrix and these materials can be practically mold into any desired shape, which may increase the range of applications significantly.

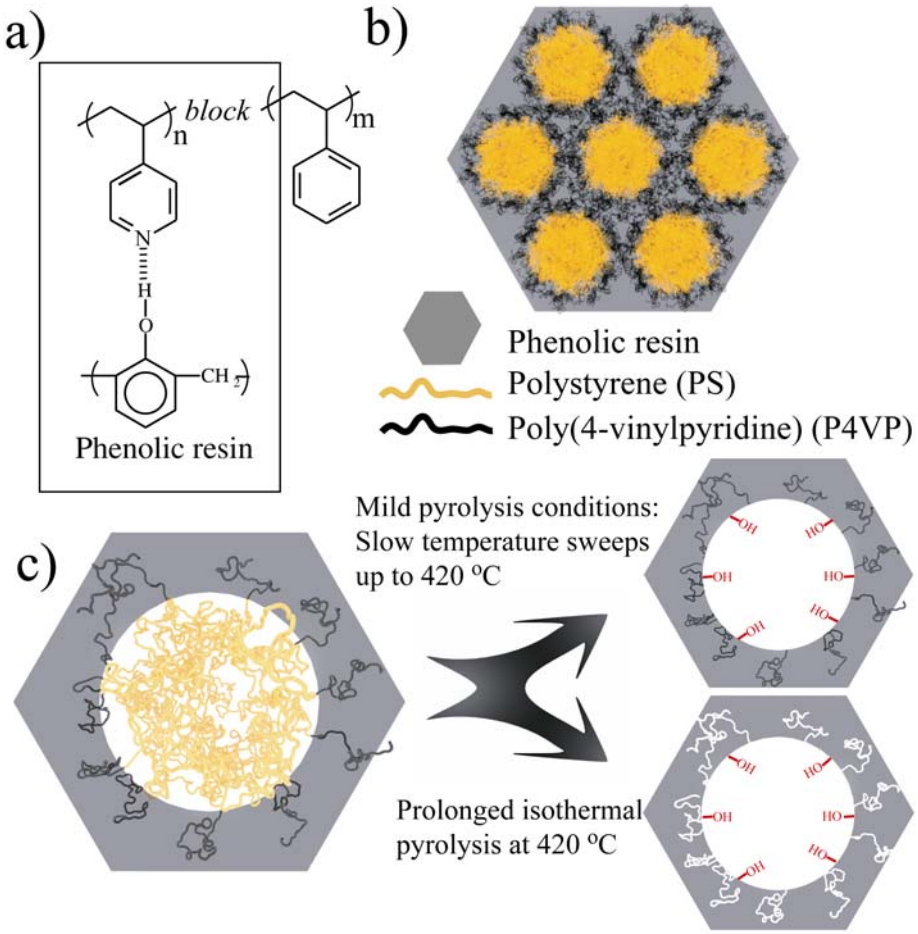

Figure 27. a) Phenolic resin, PS-*block*-P4VP and schematics of their mutual hydrogen bonding. **b)** As a result of hydrogen bonding, the phenolic resin and P4VP are confined within the same self-assembled domains as they microphase separate from the non-polar PS domains. Cross-linking at elevated temperatures "locks" the structure. **c)** During the selected pyrolysis conditions, PS-*block*-P4VP is essentially removed, leaving hierarchically porous material with a narrow distribution of pore sizes, high surface area per volume unit and hydroxyl groups at the matrix and pore walls.

The structures were analyzed using SAXS and TEM. Figure 28a shows the SAXS intensity patterns after different pyrolysis conditions and for the reference samples. Pure phenolic resin shows no intensity maximum in the measured q range, whereas cylindrical structure was obtained for the samples before and after pyrolysis. Well-defined cylindrical pores were also observed in TEM images, as illustrated in Figure 28b. For the sample pyrolyzed at 420 °C for 120 minutes the first intensity maximum and its higher order reflections are shifted to slightly higher q values, probably owing to the partial collapse of the cylindrical pores at prolonged isothermal pyrolysis, which was also suggested in TEM (Figure 28c).

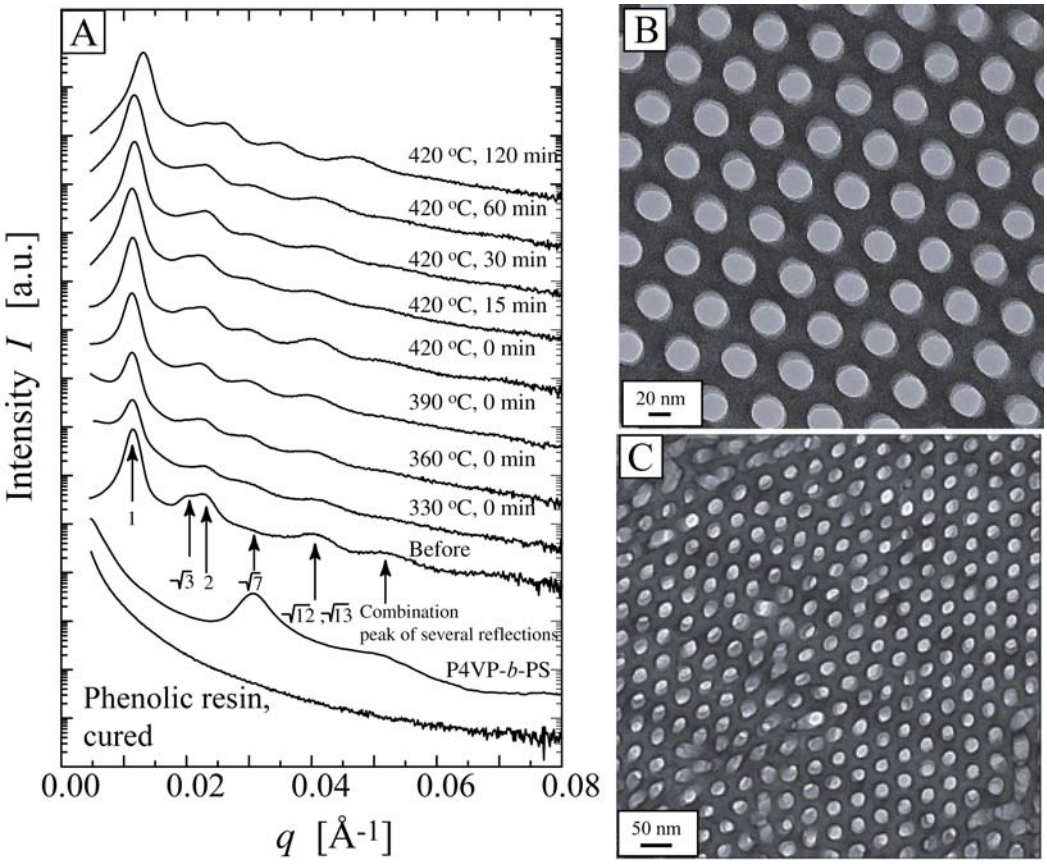

Figure 28 a) SAXS intensity patterns with different pyrolysis conditions as well as for the pure phenolic resin, pure PS-*block*-P4VP and for the sample before pyrolysis. **b)** TEM images after pyrolysis at 420 °C for 60 min and **c)** at 420 °C for 120 min.

The existence of microporous structure resulting from the P4VP chains within the phenolic matrix could not be clearly verified by conventional TEM. Thus 3D transmission electron tomography (3D-TEM), positron annihilation lifetime spectroscopy (PALS) and surface area measurements were performed. Figure 29 represents a 3D-tomogram for the sample pyrolyzed at 420 °C for 60 minutes suggesting the microporous structure within the phenolic matrix. In addition, the porosity seems to be denser close to the mesopores, which is quite reasonable.

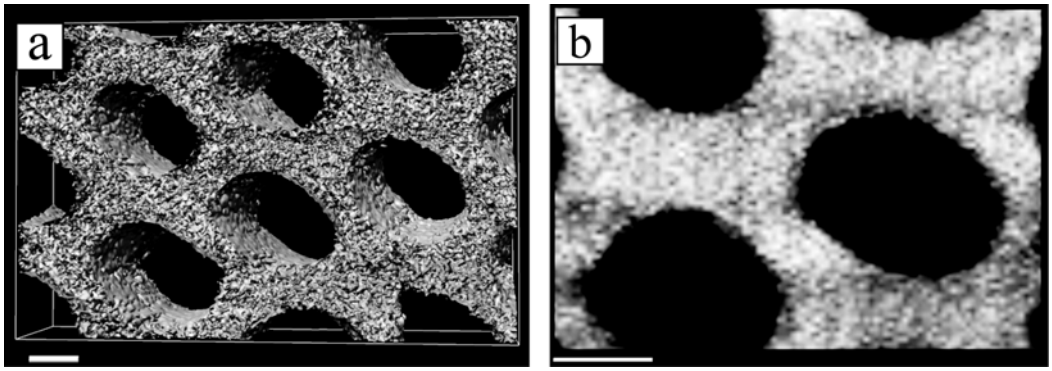

Figure 29. a) 3D-tomogram of microtomed thin section (50 nm) for the sample pyrolyzed at 420 °C for 60 minutes showing the surface roughness due to the microporous structure. **b)** 1 nm thick digital section of a selected area of tomogram rendered in solid mode. Figure reveals the micropores shown as black dots in the material. The scale bar is in both images 20 nm.

The strongest evidence for the formation of hierarchical porosity was provided by the surface area measurements (Figure 30a). Up to ca. T = 420 °C the surface area values remain relatively low resulting mainly from the mesoscale porosity. After 15 minutes isothermal pyrolysis at T = 420 °C the mesoscale surface area is leveled off to ca. 100 m^2 g^{-1}. However, the surface area owing to the microporosity increases drastically up to 500 m^2 g^{-1} during the isothermal pyrolysis period, as P4VP chains are removed from the phenolic matrix, leading to a hierarchical micro-mesoporous material. The hierarchy of porosity was also reflected to the absorption properties, where the samples with high surface area values absorbed dye from the solution much faster and the absorption was not leveled off even after 6 months (Figure 30b).

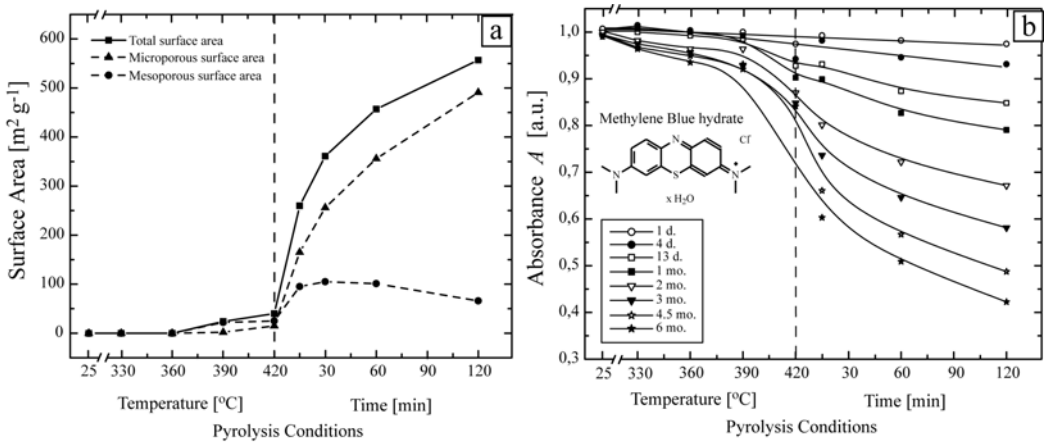

Figure 30. a) The BET surface area as a function of pyrolysis conditions. **b)** Methylene Blue (MB) concentration in aqueous solutions as a function of time upon addition to hierarchically porous phenolic absorbents in the solutions. Concentration of MB is based on its characteristic UV-Vis absorption at λ = 665 nm as a function of time.

5. CONCLUSION

In this Thesis various physical interactions are used to prepare self-assembled comb-shaped supramolecules with functional properties. The hierarchical self-assembly and phase transitions of comb-coil supramolecules consisting of hydrogen bonded side chains are described in Article I. The phase transitions are based on changes in volume fractions induced by the reversibility of the hydrogen bonding and polymer-solvent phase behavior. This enables to achieve order-order transition sequences (in some cases even 5 consecutive phase transitions) that are not easily accessible only by changing the Flory-Huggins interaction parameter χ, i.e., for example transitions from a lamellar to spherical structure. Article II describes a method to combine different physical interactions to form cylindrical self-assembly of multicomb polymeric supramolecules, in which several alkyl chains are connected to each polymeric repeat unit using both coordination and ionic interactions. As the counterions are also used as structure forming agents, this concept opens a possible platform to tune self-assembled morphologies in a rational manner.

The comb-shaped architecture leads to stretching of chains and the amphiphilic side chains act as plastizicers providing better local structures even with high molecular weight samples. In Articles III – IV we describe that these concepts can be used to prepare photonic bandgap materials. Article V, in turn, represents a system, where the reversibility of hydrogen bonding and polymer-additive phase behavior are utilized to prepare a switchable photonic bandgap material. This material shows in solid state a reversible and large bandgap switching (> 100 nm) in a narrow temperature range (< 15 ^{o}C) owing to the collapse of long period.

The use of physical interactions instead of covalent enables the cleavage of entities once the structure is formed, leading to e.g. porous materials. Articles VI – VIII describe two different template-assisted approaches towards functional porous materials: selective extraction of coordinated amphiphiles and controlled pyrolysis of block copolymer in the presence of phenolic resin. A stronger physical interaction between the amphiphiles and diblock polymer (coordination bonding) is used in Article VI, which allows using higher molecular weight amphiphiles and offers a wider variety of amphiphiles. A lamellar mesoporous structure was observed after selective removal of amphiphiles, where the glassy polystyrene domains, the different orientations of the nonaligned lamellae, and the relatively high number of defects stabilize the structure and prevent it from collapsing, leaving at least partially open pores.

In Article VII porous materials were prepared using controlled pyrolysis of templates of block copolymer and phenolic resin. The relative weight fractions of the domains were selected to obtain different morphologies, such as spherical, cylindrical, and lamellar. These materials showed a narrow distribution of pore sizes, high density of pores, relatively large surface area per volume unit, and selective absorption properties.

In Article VIII we described an approach to prepare hierarchical porous materials and tune the porosity simply by controlling the post-process conditions. The block copolymer template was selectively removed by varying pyrolysis conditions: moderate pyrolysis conditions lead to monomodal mesoporous materials, as essentially only the PS block is removed, whereas during prolonged isothermal at 420 ^{o}C also the P4VP block is removed leading to hierarchical micro-mesoporous structures with high surface area values (560 m^2 g^{-1}). In addition, the controlled pyrolysis leaves phenolic hydroxyl groups at the pore walls and matrix and these materials can be practically mold into any desired shape, which may significantly increase the range of applications.

REFERENCES

[1] Babloyantz, A., *Molecules, Dynamics, and Life: An Introduction to Self-Organization of Matter,* John Wiley & Sons, New York, 1986.

[2] Camazine, S.; Deneubourg, J.-L.; Franks, N. R.; Sneyd, J.; Theraulaz, G.; Bonabeau, E., *Self-Organization in Biological Systems,* Princeton University Press, Princeton, 2001.

[3] Whitesides, G. M.; Grzybowski, B., *Self-assembly at All Scales,* Science, **2002,** 295, 2418.

[4] Platé, N. A.; Shibaev, V. P., *Comb-Shaped Polymers and Liquid Crystals,* Plenum Press, New York and London, 1987.

[5] Agnew, N. H., *Transition Metal Complexes of Poly(vinylpyridines),* J. Polym. Sci., Polym. Chem. Ed., **1976,** 14, 2819.

[6] Martin, C. R., *Membrane-Based Synthesis of Nanomaterials,* Chem. Mater., **1996,** 8, 1739.

[7] Vögtle, F., *Supramolecular Chemistry,* John Wiley & Sons, Chichester, 1993.

[8] Ikkala, O.; Ruokolainen, J.; ten Brinke, G.; Torkkeli, M.; Serimaa, R., *Mesomorphic State of Poly(vinylpyridine)-Dodecylbenzenesulphonic Acid Complexes in Bulk and in Xylene Solution,* Macromolecules, **1995,** 28, 7088.

[9] Beginn, U., *Supramolecular Templates as Porogens,* Adv. Mater., **1998,** 10, 1391.

[10] Antonietti, M.; Burger, C.; Effing, J., *Mesomorphous Polyelectrolyte-Surfactant Complexes,* Adv. Mater., **1995,** 7, 751.

[11] Antonietti, M.; Conrad, J., *Synthesis of Highly Ordered Liquid Crystalline Phases by Complex Formation of Polyacrylic Acid with Cationic Surfactants,* Angew. Chem. Int. Ed. Engl., **1994,** 33, 1869.

[12] Antonietti, M.; Conrad, J.; Thünemann, A., *Polyelectrolyte-Surfactant Complexes: A New Type of Solid Mesomorphous Material,* Macromolecules, **1994,** 27, 6007.

[13] Hamley, I. W., *The Physics of Block Copolymers,* Oxford University Press, Oxford, 1998.

[14] Hadjichristidis, N.; Pispas, S.; Floudas, G., *Block Copolymers: Synthetic Strategies, Physical Properties, and Applications,* Wiley, 2002.

[15] Holden, G.; Kricheldorf, H. R.; Quirk, R. P., *Thermoplastic Elastomers*. 3rd ed., Hanser, Munich, 2004.

[16] Bates, F. S.; Fredrickson, G. H., *Block Copolymers - Designer Soft Materials,* Phys. Today, **1999,** 52, 32.

[17] Bates, F. S.; Fredrickson, G. H., *Block Copolymer Thermodynamics: Theory and Experiment,* Annual Review of Physical Chemistry, **1990,** 41, 525.

[18] Zheng, W.; Wang, Z.-G., *Morphology of ABC Triblock Copolymers,* Macromolecules, **1995,** 28, 7215.

[19] Adams, J.; Gronski, W., *LC Side Chain AB-Block Copolymers with an Amorphous A-Block and a Liquid-Crystalline B-Block,* Macromol. Chem., Rapid Commun., **1989,** 10, 553.

[20] Fischer, H.; Poser, S., *Liquid Crystalline Block and Graft Copolymers,* Acta Polymer, **1996,** 47, 413.

[21] Mao, G.; Ober, C. K., *Block Copolymers Containing Liquid Crystalline Segments - an Overview,* Acta Polymerica, **1997,** 48, 405.

[22] Hadjichristidis, N.; Pitsikalis, M.; Pispas, S.; Iatrou, H., *Polymers with Complex Architecture by Living Anionic Polymerization,* Chem. Rev., **2001,** 101, 3747.

[23] Hawker, C. J.; Russell, T. P., *Block Copolymer Lithography: Merging "Bottom-Up" with "Top-Down" Processes,* MRS Bulletin, **2005,** 30, 952.

[24] Lehn, J.-M., *Supramolecular Chemistry,* VCH, Weinheim, 1995.

[25] Thünemann, A. F., *Polyelectrolyte–Surfactant Complexes (Synthesis, Structure and Materials Aspects),* Prog. Polym. Sci., **2002,** 27, 1473.

[26] Zhou, S.; Chu, B., *Assembled Materials: Polyelectrolyte-Surfactant Complexes,* Adv. Mater., **2000,** 12, 545.

[27] Faul, C. F. J.; Antonietti, M., *Ionic self-assembly: Facile Synthesis of Supramolecular Materials,* Adv. Mater., **2003,** 15, 673.

[28] Antonietti, M.; Burger, C.; Thünemann, A., *Polyelectrolyte-Surfactant Complexes: A New Class of Highly Ordered Polymer Materials,* Trends in Polym. Sci., **1997,** 5, 262.

[29] Ober, C. K.; Wegner, G., *Polyelectrolyte-Surfactant Complexes in the Solid State: Facile Building Blocks for Self-Organizing Materials,* Adv. Mater., **1997,** 9, 17.

[30] Nandan, B.; Lee, C.-H.; Chen, H.-L.; Chen, W.-C., *Molecular Architecture Effect on the Microphase Separation in Supramolecular Comp-Coil Complexes of Polystyrene-block-poly(2-vinylpyridine) with Dodecylbenzenesulfonic Acid: $(AB)_nA_n$ Block-Arm Star Copolymer,* Macromolecules, **2005,** 38, 10117.

[31] Antonietti, M., *Nanostructured Materials: Self-Organization of Functional Polymers,* Nat. Mater., **2003,** 2, 9.

[32] Bazuin, C. G.; Brandys, F. A., *Novel Liquid-Crystalline Polymeric Materials via Noncovalent "Grafting",* Chem. Mater., **1992,** 4, 970.

[33] Wegner, G., *A Survey on Structure and Properties of Polymers with Metal Like Conductivity,* Makromol. Chem., Macromol. Symp., **1986,** 1, 151.

[34] Iwasaki, K.; Hirao, A.; Nakahama, S., *Morphology of Blends of α,ω-Diaminopolystyrene with α,ω-Dicarboxypoly(ethylene oxide),* Macromolecules, **1993,** 26, 2126.

[35] Bazuin, C. G.; Tork, A., *Generation of Liquid Crystalline Polymeric Materials from Non Liquid Crystalline Components via Ionic Complexation,* Macromolecules, **1995,** 28, 8877.

[36] Zheng, W.-Y.; Wang, R.-H.; Levon, K.; Rong, Z. Y.; Taka, T.; Pan, W., *Self-Assembly of the Electroactive Complexes of Polyaniline and Surfactant,* Makromol. Chem. Phys., **1995,** 196, 2443.

[37] Brandys, F. A.; Bazuin, C. G., *Mixtures of an Acid-Functionalized Mesogen with Poly(4-vinylpyridine),* Chem. Mater., **1996,** 8, 83.

[38] van der Sanden, M. C. M.; Yang, C. Y.; Smith, P.; Heeger, A. J., *Counter-Ion Induced Processibility of Conjugated Polyquinolines,* Synth. Met., **1996,** 78, 47.

[39] Antonietti, M.; Wenzel, A., *Superstructures of Lipid Bilayrs by Complexation with Helical Biopolymers,* Adv. Mater., **1997,** 9, 487.

[40] Antonietti, M.; Henke, S.; Thünemann, A., *Highly Ordered Materials with Ultra-Low Surface Energies. Polyelectrolyte-Surfactant Complexes with Fluorinated Surfactants,* Adv. Mater., **1996,** 8, 41.

[41] Chen, H.-L.; Hsiao, M.-S., *Self-Assembled Mesomorphic Complexes of Branched Poly(ethyleneimine) and Dodecylbenzenesulfonic Acid,* Macromolecules, **1999,** 32, 2967.

[42] Knaapila, M.; Ruokolainen, J.; Torkkeli, M.; Serimaa, R.; Horsburgh, L.; Monkman, A. P.; Bras, W.; ten Brinke, G.; Ikkala, O., *Self-organized Supramolecules of Poly(2,5-pyridinediyl),* Synth. Met., **2001,** 121, 1257.

[43] Peiffer, P. D.; Duvdevani, I.; P.K.Agarwal. *Transition Metal Coordination for Complexing Polymer Blends,* J. Polym. Sci., Polym. Lett. Ed., **1986,** 24, 581.

[44] Ruokolainen, J.; Tanner, J.; ten Brinke, G.; Ikkala, O.; Torkkeli, M.; Serimaa, R., *Poly(4-vinylpyridine)/Zinc Dodecyl Benzene Sulphonate. Mesomorphic State due to Coordination Complexation,* Macromolecules, **1995,** 28, 7779.

[45] Valkama, S.; Ruotsalainen, T.; Kosonen, H.; Ruokolainen, J.; Torkkeli, M.; Serimaa, R.; ten Brinke, G.; Ikkala, O., *Amphiphiles Coordinated to Block Copolymers as a Template for Mesoporous Materials,* Macromolecules, **2003,** 36, 3986.

[46] Belfiore, L. A.; Pires, A. T. N.; Wang, Y.; Graham, H.; Ueda, E., *Transition-Metal Coordination in Polymer Blends and Model Systems,* Macromolecules, **1992,** 25, 1411.

[47] Kurth, D. G.; Fromm, K. M.; Lehn, J.-M., *Hydrogen-Bonding and Metal-Ion-Mediated Self-Assembly of a Nanoporous Crystal Lattice,* Eur. J. Inorg. Chem., **2001,** 6, 1523.

[48] Gohy, J.-F.; Lohmeijer, B. G. G.; Schubert, U. S., *Reversible Metallo-Supramolecular Block Copolymer Micelles Containing a Soft Core,* Macromol. Rapid Commun., **2002,** 23, 555.

[49] Gohy, J.-F.; Lohmeijer, B. G. G.; Varshney, S. K.; Decamps, B.; Leroy, E.; Boileau, S.; Schubert, U. S., *Stimuli-Responsive Aqueous Micelles from an ABC Metallo-Supramolecular Triblock Copolymer,* Macromolecules, **2002,** 35, 9748.

[50] Ikkala, O.; ten Brinke, G., *Functional Materials Based on Self-Assembly of Polymeric Supramolecules,* Science, **2002,** 295, 2407.

[51] Ruokolainen, J.; Mäkinen, R.; Torkkeli, M.; Mäkelä, T.; Serimaa, R.; ten Brinke, G.; Ikkala, O., *Switching Supramolecular Polymeric Materials with Multiple Length Scales,* Science, **1998,** 280, 557.

[52] Ruokolainen, J.; Saariaho, M.; Ikkala, O.; ten Brinke, G.; Thomas, E. L.; Torkkeli, M.; Serimaa, R., *Supramolecular Routes to Hierarchical Structures: Comb-Coil Diblock Copolymers Organized With Two Length Scales,* Macromolecules, **1999,** 32, 1152.

[53] Ruokolainen, J.; ten Brinke, G.; Ikkala, O. T., *Supramolecular Polymeric Materials with Hierarchical Structure-within-Structure Morphologies,* Adv. Mater., **1999,** 11, 777.

[54] Thünemann, A. F.; General, S., *Poly(ethylene oxide)-b-poly(ethylene imine) Dodecanoate Complexes: Lamellar-within-lamellar Morphologies and Nanoparticles,* Macromolecules, **2001,** 34, 6978.

[55] Ruokolainen, J.; ten Brinke, G.; Ikkala, O.; Torkkeli, M.; Serimaa, R., *Mesomorphic Structures in Flexible Polymer-Surfactant Systems Due to Hydrogen Bonding: Poly(4-vinylpyridine)-Pentadecylphenol,* Macromolecules, **1996,** 29, 3409.

[56] Brunsveld, L.; Folmer, B. J. B.; Meijer, E. W.; Sijbesma, R. P., *Supramolecular Polymers,* Chem. Rev., **2001,** 101, 4071.

[57] Sijbesma, R. P.; Meijer, E. W., *Quadruple Hydrogen Bonded Systems,* Chem. Commun., **2003**, 5.

[58] Kato, T., *Self-Assembly Of Phase-Segregated Liquid Crystal Structures,* Science, **2002,** 295, 2414.

[59] Kato, T.; Mizoshita, N.; Kishimoto, K., *Functional Liquid-Crystalline Assemblies: Self-Organized Soft Materials,* Angew. Chem. Int. Ed. Engl., **2006,** 45, 38.

[60] Kato, T.; Fréchet, J. M. J., *Stabilization of Liquid-Crystalline Phase through Noncovalent Interaction with a Polymer Side Chain,* Macromolecules, **1989,** 22, 3818.

[61] Kato, T.; Fréchet, J. M. J., *Stabilization of Liquid-Crystalline Phase through Noncovalent Interaction with a Polymer Side Chain [Erratum to Document Cited in CA111(16):135185v],* Macromolecules, **1990,** 23, 360.

[62] Valkama, S.; Lehtonen, O.; Lappalainen, K.; Kosonen, H.; Castro, P.; Repo, T.; Torkkeli, M.; Serimaa, R.; ten Brinke, G.; Leskelä, M.; Ikkala, O., *Multicomb Polymeric Supramolecules and Their Self-Organization: Combination of Coordination and Ionic Interactions,* Macromol. Rapid Commun., **2003,** 24, 556.

[63] Antonietti, M.; Wenzel, A.; Thünemann, A., *The "Egg-Carton" Phase: a New Morphology of Complexes of Polyelectrolytes with Natural Lipid Mixtures,* Langmuir, **1996,** 12, 2111.

[64] Ruokolainen, J.; Tanner, J.; Ikkala, O.; ten Brinke, G.; Thomas, E. L., *Direct Imaging of Self-Organized Comb Copolymer-like Systems Obtained by Hydrogen Bonding: Poly(4-vinyl pyridine)-4-Nonadecylphenol,* Macromolecules, **1998,** 31, 3532.

[65] Ruokolainen, J.; Torkkeli, M.; Serimaa, R.; Komanschek, E.; Ikkala, O.; ten Brinke, G., *Order-Disorder Transitions in Polymer-Surfactant Systems,* Phys. Rev. E, **1996,** 54, 6646.

[66] Ruokolainen, J.; Torkkeli, M.; Serimaa, R.; Komanschek, E. B.; ten Brinke, G.; Ikkala, O., *Order-Disorder Transition in Comb-like Copolymers Obtained by Hydrogen Bonding Between Homopolymers and End-Functionalized Oligomers: Poly(4-vinyl pyridine) - Pentadecyl Phenol,* Macromolecules, **1997,** 30, 2002.

[67] Antonietti, M.; Maskos, M., *Fine-Tuning of Phase Structures and Thermoplasticity of Polyelectrolyte-Surfactant Complexes: Copolymers of Ionic Monomers with N-Alkylacrylamides,* Macromolecules, **1996,** 29, 4199.

[68] Kumar, U.; Kato, T.; Fréchet, J. M. J., *Use of intermolecular hydrogen bonding for the induction of liquid crystallinity in the side chain of polysiloxanes,* J. Am. chem. soc., **1992,** 114, 6630.

[69] Navarro-Rodriguez, D.; Guillon, D.; Skoulios, A.; Frére, Y.; Gramain, P., *Structural Behavior of Thermotropic Liquid Crystals from Poly(4-Vinylpyridine) Fully and Partially Quaternized With a Mesogenic Group,* Macromol. Chem., **1992,** 193, 3117.

[70] Tal'roze, R. V.; Platé, N. A., *Specific Interactions in Mesomorphic Self-Organized Polymeric Systems,* Polymer Sci., **1994,** 36, 1479.

[71] Kato, T.; Fréchet, J. M. J., *Hydrogen Bonding and the Self-Assembly of Supramolecular Liquid-Crystalline Materials,* Macromol. Symp., **1995,** 98, 311.

[72] Valkama, S.; Ruotsalainen, T.; Nykänen, A.; Laiho, A.; Kosonen, H.; ten Brinke, G.; Ikkala, O.; Ruokolainen, J., *Self-Asssembled Structures in Diblock Copolymers with Hydroge-Bonded Amphiphilic Plasticizing Compounds,* Macromolecules, in press.

[73] Osuji, C.; Chao, C.-Y.; Bita, I.; Ober, C. K.; Thomas, E. L., *Temperature-Dependent Photonic Bandgap in a Self-Assembled Hydrogen-Bonded Liquid-Crystalline Diblock Copolymer,* Adv. Funct. Mater., **2002,** 12, 753.

[74] Osuji, C.; Ferreira, B. J.; Mao, G.; Ober, C. K.; Vander Sande, J. B.; Thomas, E. L., *Alignment of Self-Assembled Hierarchical Microstructure in Liquid Crystalline Diblock Copolymers Using High Magnetic Fields,* Macromolecules, **2004,** 37, 9903.

[75] Ikkala, O.; ten Brinke, G., *Hierarchical Self-Assembly in Polymeric Complexes: Towards Functional Materials,* Chem. Comm., **2004**, 2131.

[76] Muthukumar, M.; Ober, C. K.; Thomas, E. L., *Competing Interactions and Levels of Ordering in Self-Organizing Polymeric Materials,* Science, **1997,** 277, 1225.

[77] Goldacker, T.; Abetz, V.; Stadler, R.; Erukhimovich, I.; Leibler, L., *Non-Centrosymmetric Superlattices in Block Copolymer Blends,* Nature, **1999,** 398, 137.

[78] Percec, V.; Ahn, C.-H.; Ungar, G.; Yeardley, D. J. P.; Möller, M.; Sheiko, S. S., *Controlling Polymer Shape Through the Self-Assembly of Dendritic Side-Groups,* Nature, **1998,** 391, 161.

[79] Manners, I., *Putting Metals into Polymers,* Science, **2001,** 294, 1664.

[80] Rehahn, M., *Organic/Inorganic Hybrid Polymers,* Acta Polym, **1998,** 49, 201.

[81] Schubert, U. S.; Eschbaumer, C., *Macromolecules Containing Bipyridine and Terpyridine Metal Complexes: Towards Metallosupramolecular Polymers,* Angew. Chem. Int. Ed. Engl., **2002,** 41, 2892.

[82] Sijbesma, R. P.; Beijer, F. H.; Brunsveld, L.; Folmer, B. J. B.; Hirschberg, J. H. K. K.; Lange, R. F. M.; Lowe, J. K. L.; Meijer, E. W., *Reversible Polymers Formed from Self-Complementary Monomers Using Quadruple Hydrogen Bonding,* Science, **1997,** 278, 1601.

[83] Kurth, D. G.; Lehmann, P.; Schütte, M., *A Route to Hierarchical Materials Based on Complexes of Metallo-Supramolecular Polyelectrolytes and Amphiphiles,* Proc. Natl. Acad. Sci. U. S. A., **2000,** 97, 5704.

[84] Pfaadt, M.; Moessner, G.; Pressner, D.; Valiyaveettil, S.; Boeffel, C.; Müllen, K.; Spiess, H. W., *Molecular Order and Dynamics of Liquid Crystals formed from Hydrogen-bonded Networks of 5-Octadecylisophtalic acid,* J. Mater. Chem., **1995,** 5, 2195.

[85] Mäki-Ontto, R.; de Moel, K.; de Odorico, W.; Ruokolainen, J.; Stamm, M.; ten Brinke, G.; Ikkala, O., *"Hairy Tubes": Mesoporous Materials Containing Hollow Self-Organized Cylinders with Polymer Brushes at the Walls,* Adv. Mater., **2001,** 13, 117.

[86] Knaapila, M.; Ikkala, O.; Torkkeli, M.; Jokela, K.; Serimaa, R.; Dolbnya, I. P.; Bras, W.; ten Brinke, G.; Horsburgh, L. E.; Pålsson, L.-O.; Monkman, A. P., *Polarized Luminescence from Self-Assembled, Aligned, and Cleaved Supramolecules of Highly Ordered Rod-Like Polymers,* Appl. Phys. Lett., **2002,** 81, 1489.

[87] Kosonen, H.; Ruokolainen, J.; Knaapila, M.; Torkkeli, M.; Jokela, K.; Serimaa, R.; ten Brinke, G.; Bras, W.; Monkman, A. P.; Ikkala, O., *Nanoscale Conducting Cylinders Based on Self-Organization of Hydrogen Bonded Polyaniline Supramolecules,* Macromolecules, **2000,** 33, 8671.

[88] Kosonen, H.; Valkama, S.; Ruokolainen, J.; ten Brinke, G.; Ikkala, O., *Polymeric One-Dimensional Reflectors Based on Self-Organization of Comb-Shaped Supramolecules,* Mat. Res. Soc. Symp. Proc., **2003,** 775, 147.

[89] Kosonen, H.; Valkama, S.; Ruokolainen, J.; Torkkeli, M.; Serimaa, R.; ten Brinke, G.; Ikkala, O., *One-Dimensional Optical Reflectors Based on Self-Organization of Polymeric Comb-Shaped Supramolecules,* Eur. Phys. J. E. Soft Matter, **2003,** 10, 69.

[90] Valkama, S.; Kosonen, H.; Ruokolainen, J.; Torkkeli, M.; Serimaa, R.; ten Brinke, G.; Ikkala, O., *Self-Assembled Polymeric Solid Films with Temperature-Induced Large and Reversible Photonic Bandgap Switching,* Nat. Mater., **2004,** 3, 872.

[91] Agarwal, P. K.; Duvdevani, I.; Peiffer, D. G.; Lundberg, R. D., *Polymer Blend Complexes Based on Coordination Chemistry,* J. Polym. Sci., Polym. Phys. Ed., **1987,** 25, 839.

[92] *From Dynamics to Devices: Directed Self-Assembly of Colloidal Materials,* MRS Bulletin, **1998,** 23.

[93] Chow, E.; Grot, A.; Mirkarimi, L. W.; Sigalas, M.; Girolami, G., *Ultracompact Biochemical Sensor Built with Two-Dimensional Photonic Crystal Microcavity,* Optics Lett., **2004,** 29, 1093.

[94] Joannopoulos, J. D., *Self-Assembly Lights Up,* Nature, **2001,** 404, 257.

[95] Joannopoulos, J. D.; Meade, R. D.; Winn, J. N., *Photonic Crystals,* Princeton University Press, Princeton, 1995.

[96] John, S., *Strong Localization of Photons in Certain Dirordered Dielectric Superlattices,* Phys. Rev. Lett., **1987,** 58, 2486.

[97] Scalora, M.; Dowling, J. P.; Bowden, C. M.; Bloemer, M. J., *Optical Limiting and Switching of Ultrashort Pulses in Nonlinear Photonic Band Gap Materials,* Phys. Rev. Lett., **1994,** 73, 1368.

[98] Temelkuran, B.; Hart, S. D.; Benoit, G.; Joannopoulos, J. D.; Fink, Y., *Wavelength-Scalable Hollow Optical Fibres with Large Photonic Bandgaps for CO_2 Laser Transmission,* Nature, **2002,** 420, 650.

[99] Yablonovitch, E., *Inhibited Spontaneous Emission in Solid-State Physics and Electronics,* Phys. Rev. Lett., **1987,** 58, 2059.

[100] Yablonovitch, E., *Photonic Crystals; Towards Rational Material Design,* Nat. Mater., **2003,** 2, 648.

[101] Yoon, J.; Lee, W.; Thomas, E. L., *Self-Assembly of Block Copolymers for Photonic-Bandgap Materials,* MRS Bulletin, **2005,** 30, 721.

[102] Campbell, M.; Sharp, D. N.; Harrison, M. T.; Denning, R. G.; Turberfield, A. J., *Fabrication of Photonic Crystals for the Visible Spectrum by Holographic Lithography,* Nature, **2000,** 404, 53.

[103] Krauss, T. F.; De La Rue, R. M., *Photonic Crystals in the Optical Regime-Past, Present and Future,* Progr. Quant. Electr., **1999,** 23, 51.

[104] Noda, S.; Tomoda, K.; Yamamoto, N.; Chutinan, A., *Full Three-Dimensional Photonic Bandgap Crystals at Near-Infrared Wavelengths,* Science, **2000,** 289, 604.

[105] Qi, M.; Lidorikis, E.; Rakich, P. T.; Johnson, S. G.; Joannopoulos, J. D.; Ippen, E. P.; Smith, H. I., *A Three-Dimensional Optical Photonic Crystal with Designed Point Defects,* Nature, **2004,** 429, 538.

[106] Ullal, C. K.; Maldovan, M.; Thomas, E. L.; Chen, G.; Han, Y.-J.; Yang, S., *Photonic Crystals Through Holographic Lithography: Simple Cubic, Diamond-Like, and Gyroid-Like Structures,* Appl. Phys. Lett., **2004,** 84, 5434.

[107] Ullal, C. K.; Maldovan, M.; Wohlgemuth, M.; Thomas, E. L.; White, C. A.; Yang, S., *Triply Periodic Bicontinuous Structures Through Interference Lithography: A Level-Set Approach,* J. Opt. Soc. Am. A, **2003,** 20, 948.

[108] Lu, Y.; Yin, Y.; Xia, Y., *Three-Dimensional Photonic Crystals with Non-spherical Colloids as Building Blocks,* Adv. Mater., **2001,** 13, 409.

[109] Gates, B.; Park, S. H.; Xia, Y., *Tuning the Photonic Bandgap Properties of Crystalline Arrays of Polystyrene Beads by Annealing at Elevated Temperature,* Adv. Mater., **2000,** 12, 653.

[110] Gates, B.; Xia, Y., *Photonic Band-Gap Properties of Opaline Lattices of Spherical Colloids Doped with Various Concentrations of Smaller Colloids,* Appl. Phys. Lett., **2001,** 78, 3178.

[111] John, S.; Busch, K., *Photonic Bandgap Formation and Tunability in Certain Self-Organizing Systems,* J. Lightwave Technol., **1999,** 17, 1931.

[112] Müller, M.; Zentel, R.; Maka, T.; Romanov, S. G.; Sotomayor Torres, C. M., *Dye-Containing Polymer Beads as Photonic Crystals,* Chem. Mater., **1999,** 12, 2508.

[113] Satoh, S.; Kajii, H.; Kawagishi, Y.; Fujii, A.; Ozaki, M.; Yoshino, K., *Tunable Optical Stop Band Utilizing Thermochromism of Synthetic Opal Infiltrated with Conducting Polymer,* Jpn. J. Appl.Phys., **1999,** 38, L1475.

[114] Xia, Y.; Yin, Y.; Lu, Y.; McLellan, J., *Template-Assisted Self-Assembly of Spherical Colloids Into Complex and Controllable Structures,* Adv. Funct. Mater., **2003,** 13, 907.

[115] Yoshino, K.; Kawagishi, Y.; Ozaki, M.; Kose, A., *Mechanical Tuning of the Optical Properties of Plastic Opal as a Photonic Crystal,* Jpn. J. Appl.Phys., **1999,** 38, L786.

[116] Yoshino, K.; Kawagishi, Y.; Tatsuhara, S.; Kajii, H.; Lee, S.; Ozaki, M.; Vardeny, Z. V.; Zakhidov, A. A., *Novel Properties of Nanoscale Organic-Inorganic Systems and Photonic Crystals - Conducting Polymers in Nanoscale Periodic Structures, Microcavities and Photonic Crystals,* Superlatt. Microstruct., **1999,** 25, 325.

[117] Miguez, H.; Meseguer, F.; López, C.; López-Tejeira, F.; Sánchez-Dehesa, J., *Synthesis and Photonic Bandgap Characterization of Polymer Inverse Opals,* Adv. Mater., **2001,** 13, 393.

[118] Vlasov, Y. A.; Bo, X.-Z.; Sturm, J. C.; Norris, D. J., *On-Chip Natural Assembly of Silicon Photonic Bandgap Crystals,* Nature, **2001,** 414, 289.

[119] Zakhidov, A. A.; Baughman, R. H.; Iqbal, Z.; Cui, C.; Khayrullin, I.; Dantas, S. O.; Marti, J.; Ralchenko, V. G., *Carbon Structures with Three-Dimensional Periodicity at Optical Wavelengths,* Science, **1998,** 282, 897.

[120] Bockstaller, M.; Kolb, R.; Thomas, E. L., *Metallodielectric Photonic Crystals Based on Diblock Copolymers,* Adv. Mater., **2001,** 13, 1783.

[121] Edrington, A. C.; Urbas, A. M.; DeRege, P.; Chen, C. X.; Swager, T. M.; Hadjichristidis, N.; Xenidou, M.; Fetters, L. J.; Joannopoulos, J. D.; Fink, Y.; Thomas, E. L., *Polymer-Based Photonic Crystals,* Adv. Mater., **2001,** 13, 421.

[122] Fink, Y.; Urbas, A. M.; Bawendi, M. G.; Joannopoulos, J. D.; Thomas, E. L., *Block Copolymers As Photonic Bandgap Materials,* J. Lightwave Technol., **1999,** 17, 1963.

[123] Urbas, A.; Sharp, R.; Fink, Y.; Thomas, E. L.; Xenidou, M.; Fetters, L. J., *Tunable Block Copolymer/Homopolymer Photonic Crystals,* Adv. Mater., **2000,** 12, 812.

[124] Maldovan, M.; Thomas, E. L., *Photonic Crystals: Six Connected Dielectric Networks with Simple Cubic Symmetry,* J. Opt. Soc. Am. B, **2005,** 22, 466.

[125] Maldovan, M.; Thomas, E. L.; Carter, C. W., *Layer-By-Layer Diamond-Like Woodpile Structure with a Large Photonic Band Gap,* Appl. Phys. Lett., **2004,** 84, 362.

[126] Maldovan, M.; Ullal, C. K.; Carter, W. C.; Thomas, E. L., *Exploring for 3D Photonic Bandgap Structures in the 11 F.C.C. Space Groups,* Nat. Mater., **2003,** 2, 664.

[127] Maldovan, M.; Urbas, A. M.; Yufa, N.; Carter, W. C.; Thomas, E. L., *Photonic Properties of Bicontinuous Cubic Microphases,* Phys. Rev. B, **2002,** 54, 165123.

[128] Urbas, A.; Fink, Y.; Thomas, E. L., *One-Dimensionally Periodic Dielectric Reflectors From Self-Assembled Block Copolymer-Homopolymer Blends,* Macromolecules, **1999,** 32, 4748.

[129] Urbas, A. M.; Maldovan, M.; DeRege, P.; Thomas, E. L., *Bicontinuous Cubic Block Copolymer Photonic Crystals,* Adv. Mater., **2002,** 14, 1850.

[130] Urbas, A. M.; Thomas, E. L.; Kriegs, H.; Fytas, G.; Penciu, R. S.; Economou, L. N., *Acoustic Excitations in a Self-Assembled Block Copolymer Photonic Crystal,* Phys. Rev. Lett., **2003,** 90, 108302/1.

[131] Deng, T.; Chen, C.; Honeker, C.; Thomas, E. L., *Two-Dimensional Block Copolymer Photonic Crystals,* Polymer, **2003,** 44, 6549.

[132] Fink, Y.; Winn, J. N.; Fan, S.; Chen, C.; Michel, J.; Joannopoulos, J. D.; Thomas, E. L., *A Dielectric Omnidirectional Reflector,* Science, **1998,** 282, 1679.

[133] Bockstaller, M. R.; Lapetnikov, Y.; Margel, S.; Thomas, E. L., *Size-Selective Organization of Enthalpic Compatibilized Nanocrystals in Ternary Block Copolymer/Particle Mixtures,* J. Am. Chem. Soc., **2003,** 125, 5276.

[134] Bockstaller, M. R.; Thomas, E. L., *Proximity Effects in Self-Organized Binary Particle-Block Copolymer Blends,* Phys. Rev. Lett., **2004,** 93, 166106/1.

[135] Bockstaller, M. R.; Thomas, E. L., *Optical Properties of Polymer-Based Photonic Nanocomposite Materials,* J. Phys. Chem. B, **2003,** 107, 10017.

[136] Ozaki, M.; Shimoda, Y.; Kasano, M.; Yoshino, K., *Electric Field Tuning of the Stop Band in a Liquid-Crystal-Infiltrated Polymer Inverse Opal,* Adv. Mater., **2002,** 14, 514.

[137] Fudouzi, H.; Xia, Y., *Photonic Papers and Inks: Color Writing with Colorless Materials,* Adv. Mater., **2003,** 15, 892.

[138] Holtz, J. A.; Asher, S. A., *Polymerized Colloidal Crystal Hydrogel Films As Intelligent Chemical Sensing Materials,* Nature, **1997,** 389, 829.

[139] Weissman, J. M.; Sunkara, H. B.; Tse, A. S.; Asher, S. A., *Thermally Switchable Periodicities and Diffraction from Mesoscopically Ordered Materials,* Science, **1996,** 274, 959.

[140] Valkama, S.; Kosonen, H.; Ruokolainen, J.; ten Brinke, G.; Ikkala, O., *unpublished data*.

[141] Ikkala, O.; Ruokolainen, J.; Torkkeli, M.; Tanner, J.; Serimaa, R.; ten Brinke, G., *Ordering in Self-Organizing Comb Copolymerlike Systems Obtained by Hydrogen Bonding Between Charged or Noncharged Polymers and Amphiphiles,* Colloids and Surfaces A, **1999,** 147, 241.

[142] Blanford, C. F.; Yan, H.; Schroden, R. C.; Al-Daous, M.; Stein, A., *Gems of Chemistry and Physics: Macroporous Metal Oxides with 3D Order,* Adv. Mater., **2001,** 13, 401.

[143] Polarz, S.; Antonietti, M., *Porous Materials via Nanocasting Procedures: Innovative Materials and Learning about Soft-Matter Organization,* Chem. Comm., **2002**, 2593.

[144] Yuan, Z.-Y.; Su, B.-L., *Insight into Hierarchically Meso-macroporous Structured Materials,* J. Mater. Chem., **2006,** 16, 663.

[145] Zhao, X. S., *Novel Porous Materials for Emerging Applications,* J. Mater. Chem., **2006,** 16, 623.

[146] Batten, S. R.; Robson, R., *Interpenetrating Nets: Ordered, Periodic Entanglement,* Angew. Chem. Int. Ed. Engl., **1998,** 37, 1460.

[147] Beginn, U.; Zipp, G.; Mourran, A.; Walther, P.; Möller, M., *Membranes Containing Oriented Supramolecular Transport Channels,* Adv. Mater., **2000,** 12, 513.

[148] Beginn, U.; Zipp, G.; Möller, M., *Functional Membranes Containing Ion-Selective Matrix-Fixed Supramolecular Channels,* Adv. Mater., **2000,** 12, 510.

[149] Bognitzki, M.; Hou, H.; Ishaque, M.; Frese, T.; Hellwig, M.; Schwarte, C.; Schaper, A.; Wendorff, J. H.; Greiner, A., *Polymer, Metal, and Hybrid Nano- and Mesotubes by Coating Degradable Polymer Template Fibers (TUFT process),* Adv. Mater., **2000,** 12, 637.

[150] Chui, S. S.-Y.; Lo, S. M.-F.; Charmant, J. P. H.; Orpen, A. G.; Williams, I. D., *A Chemically Functionalizable Nanoporous Material [Cu3(TMA)2(H2O)3]n,* Science, **1999,** 283, 1148.

[151] Ciesla, U.; Schüth, F., *Ordered Mesoporous Materials,* Microporous and Macroporous Materials, **1999,** 27, 131.

[152] Dinolfo, P. H.; Hupp, J. T., *Supramolecular Coordination Chemistry and Functional Microporous Molecular Materials,* Chem. Mater., **2001,** 13, 3113.

[153] Francois, B.; Pitois, O.; Francois, J., *Polymer Films with a Self-Organized Honeycomb Morphology,* Adv. Mater., **1995,** 7, 1041.

[154] Gudbjartson, H.; Biradha, K.; Poirier, K. M.; Zaworotko, M. J., *Novel Nanoporous Coordination Polymer Sustained by Self-Assembly of T-Shaped Moieties,* J. Am. Chem. Soc., **1999,** 121, 2599.

[155] Göltner, C. G.; Henke, S.; Weissenberger, M. C.; Antonietti, M., *Mesoporous Silica From Lyotropic Liquid Crystal Polymer Templates,* Angew. Chem. Int. Ed. Engl., **1998,** 37, 613.

[156] Hawker, C. J.; Hedrick, J. L.; Miller, R. D.; Volksen, W. U., *Supramolecular Approaches to Nanoscale Dielectric Foams for Advanced Microelectronic Devices,* MRS Bull., **2000,** 25, 54.

[157] Huo, Q.; Margolese, D.; Ciesla, U.; Feng, P.; Gier, T. E.; Sieger, P.; Leon, R.; Petroff, P. M.; Schüth, F.; Stucky, G. D., *Generalized Synthesis of Periodic Surfactant/Inorganic Composite Materials,* Nature, **1994,** 368, 317.

[158] Jenekhe, S. A.; Chen, X. L., *Self-Assembly of Ordered Microporous Materials from Rod-Coil Block Copolymers,* Science, **1999,** 283, 372.

[159] Jérôme, C.; Demoustier-Champagne, S.; Legras, R.; Jérôme, R., *Electrochemical Synthesis of Conjugated Polymer Wires and Nanotubules,* Chem. Eur. J., **2000,** 6, 3089.

[160] Kresge, C. T.; Leonowicz, M. E.; Roth, W. J.; Vartuli, J. C.; Beck, J. S., *Ordered Mesoporous Molecular Sieves Synthesized by a Liquid-Crystal Template Mechanism,* Nature, **1992,** 359, 710.

[161] Lee, H.-K.; Lee, K.; Ko, Y. H.; Chang, Y. J.; Oh, N.-K.; Zin, W.-C.; Kim, K., *Synthesis Of a Nanoporous Polymer with Hexagonal Channels from Supramolecular Discotic Liquid Crystals,* Angew. Chem. Int. Ed. Engl., **2001,** 40, 2669.

[162] Liu, J.; Fryxell, G. E.; Mattigod, S.; Zemanian, T. S.; Shin, Y.; Wang, L.-Q., *Synthesis and Applications of Functionalized Nanoporous Materials for Specific Adsorption,* Stud. Surf. Sci. Catal., **2000,** 129, 729.

[163] Martin, C. R.; Nishizawa, M.; Jirage, K.; Kang, M.; Lee, S. B., *Controlling Ion-Transport Selectivity in Gold Nanotubule Membranes,* Adv. Mater., **2001,** 13, 1351.

[164] Miller, S. A.; Kim, E.; Gray, D. H.; Gin, D. L., *Heterogeneous Catalysis with Cross-Linked Lyotropic Liquid Crystal Assemblies: Organic Analogues to Zeolites and Mesoporous Sieves,* Angew. Chem. Int. Ed. Engl., **1999,** 38, 3022.

[165] Monnier, A.; Schüth, F.; Huo, Q.; Kumar, D.; Margolese, D.; Maxwell, R. S.; Stucky, G. D.; Krishamurty, M.; Petroff, P.; Firouzi, A.; Janicke, M.; Chmelka, B. F., *Cooperative Formation of Inorganic-Organic Interfaces in the Synthesis of Silicate Mesostructures,* Science, **1993,** 261, 1299.

[166] Nangia, A., *Organic Nanoporous Structures,* Curr. Opin. Solid State Mater. Sci., **2001,** 5, 115.

[167] Percec, V.; Dulcey, A. E.; Balagurusamy, V. S. K.; Miura, Y.; Smidrkal, J.; Peterca, M.; Nummelin, S.; Edlund, U.; S.D., H.; Heiney, P. A.; Duan, H.; S.N., M.; Vinogradov, S. A., *Self-Assembly of Amphiphilic Dendritic Dipeptides Into Helical Pores,* Nature, **2004,** 430, 764.

[168] Russell, V. A.; Evans, C. C.; Li, W.; Ward, M. D., *Nanoporous Molecular Sandwiches: Pillared Two-Dimensional Hydrogen-Bonded Networks with Adjustable Porosity,* Science, **1997,** 276, 575.

[169] Russell, V. A.; Ward, M. D., *Molecular Crystals with Dimensionally Controlled Hydrogen-Bonded Nanostructures,* Chem. Mater., **1996,** 8, 1654.

[170] Seo, J. S.; Whang, D.; Lee, H.; Jun, S. I.; Oh, J.; Jeon, Y. J.; Kim, K., *A Homochiral Metal-Organic Porous Metarial for Enantioselective Separation and Catalysis,* Nature, **2000,** 404, 982.

[171] Simon, P. F. W.; Ulrich, R.; Spiess, H. W.; Wiesner, U., *Block Copolymer-Ceramic Hybrid Materials from Organically Modified Ceramic Precursors,* Chem. Mater., **2001,** 13, 3464.

[172] Su, C.-Y.; Yang, X.-P.; Kang, B.-S.; Mak, T. C. W., *Th-Symmetric Nanoporous Network Built of Hexameric Metallamacrocycles with Disparate Cavities for Guest Inclusion,* Angew. Chem., Int. Ed., **2001,** 40, 1725.

[173] Templin, M.; Franck, A.; Du Chesne, A.; Leist, H.; Zhang, Y.; Ulrich, R.; Schädler, V.; Wiesner, U., *Organically Modified Aluminosilicate Mesostructures from Block Copolymer Phases,* Science, **1997,** 278, 1795.

[174] Thurn-Albrecht, T.; Schotter, J.; Kästle, G. A.; Emley, N.; Shibauchi, T.; Krusin-Elbaum, L.; Guarini, K.; Black, C. T.; Tuominen, M. T.; Russell, T. P., *Ultrahigh-Density Nanowire Arrays Grown in Self-Assembled Diblock Copolymer Templates,* Science, **2000,** 290, 2126.

[175] Widawski, G.; Rawiso, B.; Francois, B., *Self-Organized Honeycomb Morphology of Star-Polymer Polystyrene Films,* Nature, **1994,** 369, 387.

[176] Xu, T.; Kim, H.-C.; DeRouchey, J.; Seney, C.; Levesque, C.; Martin, P.; Stafford, C. M.; Russell, T. P., *The Influence of Molecular Weight on Nano Porous Polymer Films,* Polymer, **2001,** 42, 9091.

[177] Muller, T.; Hulliger, J.; Seichter, W.; Weber, E.; Weber, T.; Wubbenhorst, M., *A New Organic Nanoporous Architecture: Dumb-Bell-Shaped Molecules with Guests in Parallel Channels,* Chem. Eur. J., **2000,** 6, 54.

[178] Kosonen, H.; Valkama, S.; Nykänen, A.; Toivanen, M.; ten Brinke, G.; Ruokolainen, J.; Ikkala, O., *Functional Porous Structures Based on the Pyrolysis of Cured Templates of Block Copolymer and Phenolic Resin.,* Adv. Mater., **2006,** 18, 201.

[179] Valkama, S.; Nykänen, A.; Kosonen, H.; Ramani, R.; Tuomisto, F.; Engelhardt, P.; ten Brinke, G.; Ikkala, O.; Ruokolainen, J., *Hierarchical Porosity in Self-Assembled Polymers: Post-Modification of Block Copolymer-Phenolic Resin Complexes by Pyrolysis Allows the Control of Micro- and Mesoporosity,* Adv. Funct. Mater., in press.

[180] Mao, H.; Hillmyer, M. A., *Nanoporous Polystyrene by Chemical Etching of Poly(ethylene oxide) from Ordered Block Copolymers,* Macromolecules, **2005,** 38, 4038.

[181] Mao, H.; Hillmyer, M. A., *Macroscopic Samples of Polystyrene with Ordered Three-Dimensional Nanochannels,* Soft Matter, **2006,** 2, 57.

[182] Ndoni, S.; Vigild, M. E.; Berg, R. H., *Nanoporous Materials with Spherical and Gyroid Cavities Created by Quantitative Etching of Polymethylsiloxane in Polystyrene-Polydimethylsiloxane Block Copolymers,* J. Am. Chem. Soc., **2003,** 125, 13366.

[183] Zalusky, A. S.; Olayo-Valles, R.; Wolf, J. H.; Hillmyer, M. A., *Ordered Nanoporous Polymers from Polystyrene-Polylactide Block Copolymers,* J. Am. Chem. Soc., **2002,** 124, 12761.

[184] Hartmann, M., *Hierarchical Zeolites: A Proven Strategy to Combine Shape Selectivity with Efficient Mass Transport,* Angew. Chem. Int. Ed., **2004,** 43, 5880.

[185] Zhou, Y.; Antonietti, M., *A Novel Tailored Bimodal Porous Silica with Well-Defined Inverse Opal Microstructure and Super-Microporous Lamellar Nanostructure,* Chem. Comm., **2003**, 2564.

[186] Newalkar, B. L.; Katsuki, H.; Komarneni, S., *Microwave-Hydrothermal Synthesis and Characterization of Microporous-Mesoporous Disordered Silica Using Mixed-Micellar-Templating Approach,* Microporous and Macroporous Materials, **2004,** 73, 161.

[187] Yang, C.-M.; Zibrowius, B.; Schmidt, W.; Schüth, F., *Consecutive Generation of Mesopores and Micropores in SBA-15,* Chem. Mater., **2003,** 15, 3739.

[188] Antonietti, M.; Berton, B.; Göltner, C.; Hentze, H.-P., *Synthesis of Mesoporous Silica with Large Pores and Bimodal Pore Size Distribution by Templating of Polymer Latices,* Adv. Mater., **1998,** 10, 154.

[189] Caruso, R. A.; Antonietti, M., *Silica Films with Bimodal Pore Structure Prepared by Using Membranes as Templates and Amphiphiles as Porogens,* Adv. Funct. Mater., **2002,** 12, 307.

[190] Maekawa, H.; Esquena, J.; Bishop, S.; Solans, C.; Chmelka, B. F., *Meso/Macroporous Inorganic Oxide Monoliths from Polymer Foams,* Adv. Mater., **2003,** 15, 591.

[191] Mann, S.; Burkett, S. L.; Davis, S. A.; Fowler, C. E.; Mendelson, N. H.; Sims, S. D.; Walsh, D.; Whilton, N. T., *Sol-Gel Synthesis of Organized Matter,* Chem. Mater., **1997,** 9, 2300.

[192] Sel, O.; Kuang, D.; Thommes, M.; Smarsly, B., *Principles of Hierarchical Meso- and Macropore Architectures by Liquid Crystalline and Polymer Colloid Templating,* Langmuir, **2006,** 22, 2311.

[193] Okabe, A.; Niki, M.; Fukushima, T.; Aida, T., *A Simple Route to Bimodal Mesoporous Silica via Tetrafluoroborate Ion-Mediated Hydrophobic Transformation of Template Micellar Surface,* J. Mater. Chem., **2005,** 15, 1329.

[194] Sun, J.-H.; Shan, Z.; Maschmayer, T.; Coppens, M.-O., *Synthesis of Bimodal Nanostructured Silicas with Independently Controlled Small and Large Mesopore Sizes,* Langmuir, **2003,** 19, 8395.

[195] Kuang, D.; Brezesinski, T.; Smarsly, B., *Hierarchical Porous Silica Materials with a Trimodal Pore System Using Surfactant Templates,* J. Am. Chem. Soc., **2004,** 126, 10534.

[196] Brandhuber, D.; Huesing, N.; Raab, C. K.; Torma, V.; Peterlik, H., *Cellular Mesoscopically Organized Silica Monoliths with Tailored Surface Chemistry by One-Step Drying/Extraction/Surface Modification Processes,* J. Mater. Chem., **2005,** 15, 1801.

[197] Sen, T.; Tiddy, G. J. T.; Casci, J. L.; Anderson, M. W., *One-Pot Synthesis of Hierarchically Ordered Porous-Silica Materials with Three Orders of Length Scale,* Angew. Chem. Int. Ed., **2003,** 42, 4649.

[198] Sen, T.; Tiddy, G. J. T.; Casci, J. L.; Anderson, M. W., *Synthesis and Characterization of Hierarchically Ordered Porous Silica Materials,* Chem. Mater., **2004,** 16, 2044.

[199] Hentze, H.-P.; Antonietti, M., *Template Synthesis of Porous Organic Polymers,* Curr. Opin. Solid State Mater. Sci., **2001,** 5, 343.

[200] Zhao, X. S.; Su, F.; Yan, Q.; Guo, W.; Bao, X. Y.; Lv, L.; Zhou, Z., *Templating Methods for Preparation of Porous Structures,* J. Mater. Chem., **2006,** 16, 637.

[201] Holland, B. T.; Blanford, C. F.; Stein, A., *Synthesis of Macroporous Minerals with Highly Ordered Three-Dimensional Arrays of Spheroidal Voids,* Science, **1998,** 281, 538.

[202] Velev, O. D.; Jede, T. A.; Lobo, R. F.; Lenhoff, A. M., *Porous Silica via Colloidal Crystallization,* Nature, **1997,** 389, 447.

[203] Imhof, A.; Pine, D. J., *Ordered Macroporous Materials by Emulsion Templating,* Nature, **1997,** 389, 948.

[204] Breulmann, M.; Davis, S. A.; Mann, S.; Hentze, H.-P.; Antonietti, M., *Polymer-Gel Templating of Porous Inorganic Macro-Structures Using Nanoparticle Building Block,* Adv. Mater., **2000,** 12, 502.

[205] Antonelli, D. M., *Synthesis of Macro-Mesoporous Niobium Oxide Molecular Sieves by a Ligand-Assisted Vesicle Templating Strategy,* Microporous and Macroporous Materials, **1999,** 33, 209.

[206] Sepulveda, P.; Binner, J. G. P., *Processing of Cellular Ceramics by Foaming and in situ Polymerisation of Organic Monomers,* J. Eur. Ceram. Soc., **1999,** 19, 2059.

[207] Davis, S. A.; Burkett, S. L.; Mendelson, N. H.; Mann, S., *Bacterial Templating of Ordered Macrostructures in Silica and Silica-Surfactant Mesophases,* Nature, **1997,** 385, 420.

[208] Dean, J. M.; Lipic, P. M.; Grubbs, R. B.; Cook, R. F.; Bates, F. S., *Micellar Structure and Mechanical Properties of Block Copolymer-Modified Epoxies,* J. Polym. Sci. B, Polym. Phys., **2001,** 39, 2996.

[209] Rebizant, V.; Abetz, V.; Tournilhac, F.; Court, F.; Leibler, L., *Reactive Tetrablock Copolymer Containing Glycidyl Metacrylate, Synthesis and Morphology Control in Epoxy-Amine Networks,* Macromolecules, **2003,** 36, 9889.

[210] Ritzenthaler, S.; Court, F.; David, L.; Girard-Reydet, E.; Leibler, L.; Pascault, J. P., *ABC Triblock Copolymers/Epoxy-Diamine Blends. 1. Keys to Achieve Nanostructured Thermosets,* Macromolecules, **2002,** 35, 6245.

[211] Grubbs, R. B.; Dean, J. M.; Broz, M. E.; Bates, F. S., *Reactive Block Copolymers for Modification of Thermosetting Epoxy,* Macromolecules, **2000,** 33, 9522.

[212] Hillmyer, M. A.; Lipic, P. M.; Hajduk, D.; Almdal, K.; Bates, F. S., *Self-Assembly and Polymerization of Epoxy Resin-Amphiphilic Block Copolymer Nanocomposites,* J. Am. Chem. Soc., **1997,** 119, 2749.

[213] Lipic, P. M.; Bates, F. S.; Hillmyer, M. A., *Nanostructured Thermosets from Self-Assembled Amphiphilic Block Copolymer/ Epoxy Resin,* J. Am. Chem. Soc., **1998,** 120, 8963.

[214] Lipic, P. M.; Bates, F. S.; Hillmyer, M. A., *Self-Assembly and Polymerization of Epoxy Resin-Amphiphilic Block Copolymer Nanocomposites,* J. Am. Chem. Soc., **1998,** 119, 2749.

[215] Mijovic, J.; Shen, M.; Sy, J. W.; Mondragon, I., *Dynamics and Morphology in Nanostructured Thermoset Network/Block Copolymer Blends during Network Formation,* Macromolecules, **2000,** 33, 5235.

[216] Guo, Q.; Thomann, R.; Gronski, W.; Staneva, R.; Ivanova, R.; Stühn, B., *Nanostructures, Semicrystalline Morphology, and Nanoscale Confinement Effect on the Crystallization Kinetics in Self-Organized Block Copolymer/Thermoset Blends,* Macromolecules, **2003,** 36, 3635.

[217] Guo, Q.; Thomann, R.; Gronski, W.; Thurn-Albrecht, T., *Phase Behavior, Crystallization and Hierarchical Nanostructure in Self-Organized Thermoset Blends of Epoxy Resin and Amphiphilic Poly(ethylene oxide)-block-Poly(propylene oxide)-block-Poly(ethylene oxide) Triblock Copolymers,* Macromolecules, **2002,** 35, 3133.

[218] Kosonen, H.; Ruokolainen, J.; Nyholm, P.; Ikkala, O., *Self-Organized Thermosets: Blends of Hexamethylenetetramine Cured Novolac with Poly(2-Vinylpyridine)-block-poly(isoprene),* Macromolecules, **2001,** 34, 3046.

[219] Kosonen, H.; Ruokolainen, J.; Nyholm, P.; Ikkala, O., *Self-Organized Crosslinked Phenolic Thermosets: Thermal and Dynamic Mechanical Properties of Novolac/Block Copolymer Blends,* Polymer, **2001,** 42, 9481.

[220] Kosonen, H.; Ruokolainen, J.; Torkkeli, M.; Serimaa, R.; Nyholm, P.; Ikkala, O., *Micro- and Macrophase Separation in Phenolic Resol Resin / PEO-PPO-PEO Block Copolymer Blends: Effect of Hydrogen-Bonded PEO Length,* Macromol. Chem. Phys., **2002,** 293, 388.

[221] Ganeva, D.; Antonietti, M.; Faul, C. F. J.; Sanderson, R., *Polymerization of the Organized Phases of Polyelectrolyte-Surfactant Complexes,* Langmuir, **2003,** 19, 6561.

[222] Ganeva, D.; Faul, C. F. J.; Götz, G.; Sanderson, R. D., *Directed reactions within confined reaction environments: Polyadditions in polyelectrolyte-surfactant complexes,* Macromolecules, **2003,** 36, 2862.

[223] Paleos, C. M.; Malliaris, A., *Polymerization of Micelle-Forming Surfactants,* Makromol. Chem. Phys., **1988,** C28, 403.

[224] Mittal, K.; Fendler, E. J., *Solution Behavior of Surfactants,* Plenum Press, New York, 1982.

[225] Yasuda, Y., *Polymerizable Surfactants: Spontaneous Polymerization in Organized Micellar Media,* Annual Surfactants Review, **1999,** 2, 317.

[226] Moriguchi, I.; Ozono, A.; Mikuriya, K.; Teraoka, Y.; Kagawa, S.; Kodama, M., *Micelle-Templated Mesophases of Phenol-Formaldehyde Polymer,* Chem. Lett., **1999,** 11, 1171.

[227] Liang, C.; Dai, S., *Synthesis of Mesoporous Carbon Materials via Enhanced Hydrogen-Bonding Interaction,* J. Am. Chem. Soc., **2006,** 128, 5316.

[228] Liang, C.; Hong, K.; Guiochon, G. A.; Mays, J. W.; Dai, S., *Synthesis of A Large-Scale Highly Ordered Porous Carbon Film by Self-Assembly of Block Copolymers,* Angew. Chem. Int. Ed., **2004,** 43, 5785.

[229] Mullens, J.; Yperman, J.; Francois, J. P.; Van Poucke, L. C., *Simultaneous Calorimetric Determination of Equilibrium Constant and Enthalpy Change of Hydrogen-Bond Complex in Dilute Solutions of Phenol with Pyridine in Carbon Tetrachloride,* J. Phys. Chem. , **1985,** 89, 2937.

ABSTRACTS OF PUBLICATIONS I-VIII

I Hydrogen-bonding amphiphilic low molecular weight plasticizing compounds to one block of diblock copolymers to form supramolecular comblike blocks leads to hierarchical self-assembly at the block copolymer (long) and amphiphile (short) length scales, in which lamellar-in-lamellar order and the related phase transitions have previously been shown to allow thermal switching of electrical and optical properties [*Science* **1998**, *280*, 557; *Nat. Mater.* **2004**, *3*, 872]. In this work other hierarchies and phase transitions are systematically searched, a particular interest being hierarchies containing gyroid structures and the related order-order transitions. Polymeric supramolecular comb-coil diblock copolymers consisting of a polystyrene (PS) coillike block and a supramolecular comblike block based on poly(4-vinylpyridine) (P4VP) are used, where the pyridines are either directly hydrogen bonded with 3-pentadecylphenol (PDP), i.e., PS-*block*-P4VP(PDP)$_{1.0}$, or first protonated with methanesulfonic acid (MSA) and then hydrogen bonded to PDP, i.e., PS-*block*-P4VP(MSA)$_{1.0}$(PDP)$_{1.0}$. In this way the comblike block can be noncharged or charged. The morphologies were determined using transmission electron microscopy (TEM) and small-angle X-ray scattering (SAXS) at different temperatures. In the case of PS-*block*-P4VP(PDP)$_{1.0}$, all classical diblock copolymer morphologies were observed at room temperature, where the P4VP(PDP)$_{1.0}$ domains contain an additional lamellar structure due to the supramolecular comblike blocks. Here we report novel gyroid and hexagonal perforated layer morphologies, i.e., where the PS and P4VP(PDP)$_{1.0}$ blocks form gyroid or hexagonal perforated layer order and the P4VP(PDP)$_{1.0}$ domains have an internal lamellar order. Heating past ca. T = 60 ^{o}C causes an order–disorder transition within the P4VP(PDP)$_{1.0}$ domains. Further heating leads to gradually reduced hydrogen bonding strength, and importantly PDP becomes soluble in PS at T > ca. 120 ^{o}C. At such temperatures PDP is found in both the P4VP and PS domains, thus leading to changes in the relative volume fractions of the domains, which in turn leads to order–order transitions. In PS-*block*-P4VP(MSA)$_{1.0}$(PDP)$_{1.0}$, typically lamellar and cylindrical block copolymeric structures were observed, where there was an additional internal lamellar order within the P4VP(MSA)$_{1.0}$(PDP)$_{1.0}$ domains. Coincidentally, an order–disorder transition within the P4VP(MSA)$_{1.0}$(PDP)$_{1.0}$ domains takes place at T = ca. 125 ^{o}C. Above that temperature, PDP is in both PS and P4VP(MSA)$_{1.0}$ domains, but most interestingly at ca. T > 175 ^{o}C PDP becomes a nonsolvent for P4VP(MSA)$_{1.0}$ and it is therefore expelled to predominantly to the PS domains. This manifests as an order–order transition. All samples exhibit at least two thermoreversible order–order transitions, and some of them show even five consecutive self-assembled phases as a function of temperature. Besides being amphiphilic, PDP can also be regarded as a plasticizer, i.e., relatively nonvolatile solvent, for the P4VP, PS, and P4VP(MSA)$_{1.0}$ with characteristic phase behaviors. This, in combination with the comb–coil diblock copolymer composition and the reversibility of the hydrogen bonding, enables to achieve thermoreversible transition sequences that are not easily accessible only by changing the Flory–Huggins interaction parameter χ by temperature, for example transitions from a lamellar to spherical structure. The combination of phase behaviors of self-assembly and polymer/plasticizer mixtures allows new structural hierarchies and phase transitions that may lead to new types of responsive materials.

II Several alkyl side chains are bonded to each polymeric repeat unit using both coordinated ligands and electrostatically bound counterions to directly control the interface curvature of the self-organized structures. 2,6-Bis(octylaminomethyl)pyridine is Zn-coordinated to poly(4-vinylpyridine) (P4VP) with dodecylbenzenesulfonate (DBS) counterions, leading to multicomb polymeric supramolecules, poly[(4VP)Zn(2,6-bis(octylaminomethyl)-pyridine(DBS)$_2$].

Coordination is evidenced by infrared spectroscopy and visualized by quantum chemical calculations. The amorphous hexagonal self-organized structures are characterized using X-ray measurements.

III We demonstrate that complexation of dodecylbenzenesulphonic acid, DBSA, to a diblock copolymer of polystyrene-*block*-poly(4-vinylpyridine), PS-*block*-P4VP, leads to polymeric supramolecules PS-*block*-P4VP(DBSA)$_y$ (y = 1.0, 1.5, and 2.0), which self-organize with a particularly large lamellar periodicity in excess of 1000 ˚A. The structures consist of alternating PS and P4VP(DBSA)$_y$ layers, where the latter contains smaller internal structure, probably lamellar. The DBSA side chains are bonded to the pyridines by protonation and hydrogen bonding and they effectively plasticize the material. In this way relatively well-developed structures are obtained even without annealing or macroscopic alignment. Transmission and reflectance measurements show that a relatively narrow and incomplete bandgap exists for supramolecules of high molecular weight block copolymer at ca. 460 nm.

IV Polystyrene-*block*-poly(4-vinylpyridine) (PS-*block*-P4VP) diblock copolymer was complexed with dodecylbenzenesulfonic acid (DBSA), leading to comb–coil polymeric supramolecules PS-*block*-P4VP(DBSA)$_y$ (y = 1.0, 1.5, and 2.0). Complexes formed hierarchical lamellar structure with long period of ca. 1400 Å. Due to periodicity and refractive index contrast between the layers, transmission and reflectance measurements showed a relatively narrow incomplete bandgap at ca. 460 nm. The angular dependence of the bandgap was also studied using different angles (θ) relative to the surface normal. The mid-gap was blue-shifted when the incident angle was increased indicating that the lamellar structure was partly oriented by the surfaces of quartz glasses.

V In aqueous solutions the response of polymers and biological matter to external conditions, such as temperature and pH, is typically based on the hydrophobic/hydrophilic balance and its effects on the polymer conformation. In the solid state, related concepts using competing interactions could allow novel functions. In this work we demonstrate that polymeric self-assembly, reversibility of hydrogen bonding, and polymer–additive phase behaviour allow temperature response in the solid state with large and reversible switching of an optical bandgap. A complex of polystyrene-*block*-poly(4-vinylpyridinium methanesulphonate) and 3-*n*-pentadecylphenol leads to the supramolecular comb-shaped architecture with a particularly long lamellar period. The sample is green at room temperature, as an incomplete photonic bandgap due to a dielectric reflector is formed. On heating, hydrogen bonds are broken and 3-*n*-pentadecylphenol additionally becomes soluble in polystyrene, leading to a sharp and reversible transition at ~125 °C to uncoloured material due to collapse of the long period. This encourages further developments, for example, for functional coatings or sensors in the solid state.

VI We show a concept where coordination of amphiphiles to one block of a block copolymer leads to polymeric supramolecules and self-organization and that mesoporous materials can be achieved with a dense set of polymer brushes at the surfaces upon cleaving the amphiphiles by extraction with a selective solvent. Polystyrene-*block*-poly(4-vinylpyridine) (PS-*block*-P4VP) is used with zinc dodecylbenzenesulfonate (Zn(DBS)$_2$) which can coordinate to the lone electron pairs of the pyridine nitrogens in the P4VP block, leading to complexes PS-*block*-P4VP[Zn(DBS)$_2$]$_y$. Coordination of Zn(DBS)$_2$ and structure formation were investigated using Fourier transformation infrared spectroscopy (FTIR), small- and wide-angle X-ray scattering (SAXS and WAXS), and transmission electron microscopy (TEM). Lamellar structure was observed and even points toward a structural hierarchy for high molecular weight block copolymers. FTIR, SAXS, and

TEM showed that most of $Zn(DBS)_2$ can be extracted from such templates using methanol, leading to lamellar porous structures. P4VP brushes cover the resulting pore surfaces. The structures do not collapse probably due to the glassy PS and defects in the nonaligned structure. Compared to hydrogen bonding, coordination allows bonding of higher molecular weight amphiphiles due to the stronger attraction.

VII Porous materials with controlled pore sizes have been investigated for different applications such as filters, separation, sensors, supports for catalysis, and controlled drug release. Proper selection of chemical groups lining the pore walls, as well as detailed control of the pore size and size distribution, can lead to selectivity and various functions. In this work we describe a facile method to construct porous films by crosslinking phenolic resin in the presence of a self-assembled block-copolymer template, followed by pyrolysis at moderate temperature. This enables us to transfer the ordered block copolymer self-assembly into porosity, with a fine control of the pore size and distribution. These materials have large surface area (in excess of 300 $m^2\ g^{-1}$), with a high number of phenolic hydroxyl groups at the matrix and pore walls, which can be used for, e.g., selective absorption or for further functionalization.

VIII We show that self-assembled hierarchical porosity in organic polymers can be obtained in a facile manner based on pyrolyzed block copolymer/phenolic resin nanocomposites and show that a given starting composition can be post-modified in a wide range from monomodal mesoporous materials to hierarchical micro-mesoporous materials with high density of pores and large surface area per volume unit (up to 500 - 600 $m^2\ g^{-1}$). For that purpose we use self-assembled cured composites where phenolic resin is templated by a diblock copolymer poly(4-vinylpyridine)-*block*-polystyrene (P4VP-*b*-PS). Mild pyrolysis conditions lead only to monomodal mesoscale porosity, as essentially only the PS block is removed (length scale tens of nm), whereas during more severe conditions under prolonged isothermal pyrolysis at 420 ^oC also the P4VP chains within the phenolic matrix are removed leading to additional microporosity (length scale less than nm). The porosity was analyzed using TEM, SAXS, 3D-TEM, PALS, and BET measurements. Furthermore, the relative amount of micro- and mesopores can be tuned in-situ by post modification. As controlled pyrolysis leaves phenolic hydroxyl groups at the pore walls and the thermoset resin based materials can be easily molded into desired shape, we expect that such materials could be useful for, e.g., sensors, separation materials, filters, and templates for catalysis.

ISBN-13 978-951-22-8497-9
ISBN-10 951-22-8497-9
ISBN-13 978-951-22-8498-6 (PDF)
ISBN-10 951-22-8498-7 (PDF)
ISSN 1795-2239
ISSN 1795-4584 (PDF)